Title
A Phase-Variable Surface Layer from the Human Gut Commensal Bacteroides

Author
Taketani, Mao

Publication Date
2014

Peer reviewed|Thesis/dissertation

A Phase-Variable Surface Layer from the Human Gut Commensal *Bacteroides*

By

Mao Taketani

A dissertation submitted in partial satisfaction of the

requirements for the degree of

Doctor of Philosophy

in

Infectious Diseases and Immunity

in the

Graduate Division

of the

University of California, Berkeley

Committee in Charge:

Lee W. Riley, Chair

Michael A. Fischbach

Russell E. Vance

Michi E. Taga

Fall 2014

Abstract

A Phase-Variable Surface Layer from the

Human Gut Commensal *Bacteroides*

By

Mao Taketani

Doctor of Philosophy in Infectious Diseases and Immunity

University of California, Berkeley

Professor Lee W. Riley, Chair

While some microbial encounters can be pathogenic, most interactions between humans and microorganisms do not result in disease. Our gastrointestinal tract harbors approximately 100 trillion organisms, spanning about 1000 species that live in harmony with us. While we provide them with food and shelter, this complex intestinal bacterial community supplies essential nutrients, metabolizes indigestible compounds, protects us from pathogenic organisms and helps develop our immune system, thereby establishing a symbiotic relationship. *Bacteroides* are one of the most abundant bacterial genera living in the human gut and has long been a model system for studying the molecular mechanisms of commensal-host interactions. In the course of searching for surface structures that have immunomodulatory properties on the host, we serendipitously discovered a previously unknown surface protein BT1927 from *Bacteroides* that is capable of completely covering the surface of the bacteria by creating a tessellated surface layer. Interestingly, the formation of the entire proteinaceous capsule is controlled by inversion of a single promoter, making it phase-variable. Although only ~ 0.1% of the population produce this capsule in laboratory culture, analyzing the fecal metagenome sequence data from the Human Microbiome Project revealed that ~ 8% of the population produce a homologous capsule in humans, suggesting its significance *in vivo*. From a series of functional studies, we found that the BT1927-expressing subpopulation is profoundly resistant to complement-mediated killing, due in part to the BT1927-mediated blockade of C3b deposition. Our results show that the *Bacteroides* capsule is capable of a far greater degree of structural variation than previously known, perhaps to cope with the varying environmental conditions in the human intestine.

Acknowledgements

I would like to thank my incredible boss Dr. Michael A. Fischbach for his support throughout my graduate career at UC Berkeley. Thank you for introducing me into the fascinating field of the microbiome. Thank you for believing in me so that I could work and grow as an independent scientist while providing me scientific guidance, motivation and financial support. Thank you for creating a comfortable and supportive environment for me to work in. I will continue to admire and respect you as a scientist and as a human being.

To the members of the Fischbach Lab: Jan Claesen, Sloan Devlin, Mohamed Donia, Amy Jacobson, Laurens Kraal, Aedan Liu, Colleen O'Loughlin, Tiffany Scharschmidt, Yug Varma, Brianna Williams; thank you for being so supportive throughout my graduate career, especially for the times when it was so hard to continue. I want to give a special thanks to Brianna, who has been the leading factor in making the lab a comfortable and welcoming place for everyone. Without you, the lab will never be the same. I would like to thank Mohamed, thank you for your continued support and intellectual guidance. I don't think I could have done it without you. I would also like to acknowledge Mohamed's work on the analysis of the HMP metagenome sequence data presented in this dissertation. I would also like to thank Jan, also for the continued support and helpful discussions, especially about bacterial genetics. I would like to acknowledge Amy's dedication for running many protein gels that lead to the discovery of BT1927.

My dissertation work was not possible without the help of many collaborators. Thank you Greg Barton and the rest of Barton lab for advice and technical assistance on experiments and analysis on the immunological assays conducted. I would like to especially acknowledge Meghan Koch's work on analyzing the TLR data for this dissertation. Thank you Neil Kelleher and Yunqiu Chen for amino acid analysis of BT1927; Jeff Johnson from Nevan Krogan's lab for amino acid sequencing of BT1927; John Lambris for intellectual guidance on complement experiments; Justin Sonnenburg for providing strains and plasmids as well as advice to perform genetics on *B. thetaiotaomicron* and Kristen Anne Earle for advice on FISH; Reena Zalpuri from UC Berkeley EM lab for technical assistance on TEM work.

I would like to thank my home at UC Berkeley, the Graduate Group in Infectious Diseases and Immunity for accepting me into the program. I would like to especially thank my dissertation committee chair Dr. Lee Riley for supporting me to work across the UC San Francisco and UC Berkeley campuses. Dr. Russell Vance for input on my manuscript, and Dr. Michi Taga for helpful guidance on my dissertation. I would like to thank my Qualifying Exam Committee members: Dr. George Sensabaugh, Dr. Sangwei Liu, Dr. Terry Machen, and especially Dr. Bill Sha for valuable and passionate input on my qualifying exam proposal. I would also like to thank Teresa Liu for her support as a student manager, and taking the 'mom' role in

the program.

To the fellow Infectious Diseases and Immunity Ph.D graduates: Chris Baker, Liana Chan, Danica Helb and Ebere Sonoiki, thank you for your continued friendship and support. You guys have made my experience at UC Berkeley a fun and stimulating one. Thank you Chris for also providing me technical help and guidance on the flow cytometry.

I would like to thank Arel Cordero for always being there for me.

Finally, I would like to thank my family: my mom Ritsuko Taketani, for her continuous love and support, my dad Makoto Taketani for his continued influence as a scientist, my little sister and best friend Maya Taketani, and my grandma Kazue Tanaka for her emotional support through care packages all the way from Japan.

Table of Contents

List of Figures

List of Tables

Chapter 1 : Introduction

The Human Microbiome

The human microbiome (or the microbiota) is a collection of bacteria, fungi and viruses that colonize our body in places like the skin, mouth, gut and the vagina. It is estimated that the number of bacteria that live inside our body outnumber our own cells by a factor of ten, and that there are approximately 500 to 1000 different species of bacteria that live inside us (1, 2). It has been increasingly clear that these microbial inhabitants play a significant role in our health. It is believed that a person's healthy microbiome provides homeostasis, and when this intricate balance is tipped, or in a state of *dysbiosis*, there can be negative consequences to human health (3).

Recent advances in sequencing technology have enabled researchers to decipher the composition of this complex ecosystem. In particular, next-generation sequencing technology such as the Illumina Hiseq has enabled us to understand the composition at the species level using 16S rDNA metagenomic sequencing. For example, given a fecal sample, 16S sequencing can tell us all the species that it contains, such as *Bacteroides fragilis*, *Ruminococcus gnavus* and *Clostridium scindens* species.

More recently whole-genome metagenomic sequencing has allowed us to understand the sample composition at the strain level by sequencing the entire genome of each member within a complex sample. Knowing the composition of bacteria at the strain level is integral to perform more detailed mechanistic studies. For example, Donia and coworkers systematically identified biosynthetic gene clusters from whole-genome metagenome sequence data and identified an antibiotic mediating microbe-to-microbe interaction within the vaginal microbiome (4). This would not have been possible with 16S sequencing, which does not contain information about which genes are present in the organism.

The whole-genome metagenomic sequencing technology has even allowed assembly of whole genomes of novel bacteria, which have never been isolated and characterized before. Since many members of the microbiota are unculturable (cannot be isolated and/or grown in the laboratory), this information will likely help researchers study these elusive organisms that are most likely important to our health.

The Human Microbiome Project and the MetaHIT project are examples of large scale national and international studies sponsored by the National Institute of Health, and the European Commission, respectively, to establish associations between the microbiota profile and state of human health and disease using these technologies (5–9). From these and other studies, there have been many significant associations made between the microbiome composition and clinically significant diseases including Inflammatory Bowel Disease (IBD) such as Crohn's and ulcerative colits, obesity, type 2 diabetes, atherosclerosis, allergy, autism spectrum disorder and many more (3, 10–13).

A pioneer and leader in studying the ecology of the microbiome and its effects on human health, Jeffrey Gordon's group has elegantly shown that the microbiota contributes to the pathology of obesity by reporting that the obese microbiome has an increased capacity to harvest energy from the diet (14). Furthermore, they showed that this trait is transmissible by colonizing germ-free mice with an *obese* microbiota, which resulted in a greater increase in total body fat than germ-free mice colonized with a *lean* microbiota

(15).

Another seminal experimental work presented by Stanley Hazen's group has shown that the gut microbiota has a major contribution in converting dietary choline into trimethylamine (TMA) which is rapidly metabolized by a hepatic flavin monooxygenase to produce trimethylamine N-oxide (TMAO), a proatherogenic compound unambiguously associated with high cardiovascular risk (16). Interestingly, when omnivorous human subjects ingested red meat abundant in L-carnitine, which also leads to production of TMAO, the production of TMAO was much higher than in vegans or vegetarians, suggesting that a specific member of the omnivorous microbiota is the main contributor in metabolizing L-carnitine into TMA (17).

The study which showed the therapeutic potential of the microbiota was a randomized controlled clinical trial, conducted to study the effect of fecal transplant in patients with recurring *Clostridium difficile* infection, a causative agent of antibiotic-associated pseudomembranous enterocolitis, which leads to severe diarrhea. Fecal transplant cure rate was so high (>80% for duodenal infusion in this case study, but there have been reports of >90% with colonoscopy or enema use in other studies) compared to the traditional antibiotics treatment that the trial had to be prematurely discontinued due to the fact that having untreated controls was unethical (18, 19).

The Microbiome and the Immune System

The use of germ-free animals (or gnotobiotic animals, where microbial status of the animal is known) has been a key tool in studying the effect of the microbiota on health and disease. These animals are reared in sterile isolators to control their exposure to microorganisms, and have become essential in studying the effect of single organisms or defined mixtures of organisms (20). Direct comparisons of the phenotype of germ-free animals and conventional animals have also led to early discoveries about the role of the microbiome. One striking observation is that germ-free animals do not have a fully developed immune system. They completely lack organized lymphoid structures leading to deficiency in antibodies and key immune cells in the gut required for protection from infections (21). These initial observations were followed by seminal papers showing that the microbiome plays a significant role in developing a healthy immune system.

Dan Littman's group has published seminal works reporting that a particular commensal bacteria, called the Segmented Filamentous Bacteria (SFB) present in the mouse gut is sufficient to induce production of immune cells called Th17 cells, which play a significant role in protecting the host from infections. This finding came from a striking observation that while mice purchased from Jackson Laboratory had very low numbers of Th17 cells, mice purchased from Taconic Farms had very high numbers of Th17 cells. Co-housing Jackson mice with Taconic mice, as well as transferring Taconic mice intestinal contents into Jackson mice induced the production of Th17 cells. The group screened for bacteria that were highly abundant in Taconic mice but not in Jackson mice and found that a single bacteria, SFB (only SFB and not others), was sufficient enough to induce production of Th17 cells (22, 23). Presence of SFB in the gut has been correlated with reduced abundance and growth of pathogenic bacteria (24, 25). SFB on the intestinal tissue viewed under a Scanning EM has a unique appearance, where it penetrates the

mucus layer above the epithelial cells. This close interaction, through a still unknown mechanism, is believed to result in induction of Th17 cells (22).

Germ-free mice also lack specific immune cells called regulatory T cells, which are important for downregulating and suppressing the immune response. Kenya Honda's group, in a search for a treatment of inflammatory and allergic diseases, have isolated a group of strains belonging to the *Clostridium* genus that produce an anti-inflammatory response, through induction of regulatory T cells. The group has shown that this '*Clostridium* cocktail' can attenuate the disease in colitis and allergic models when administered orally (26, 27).

Bacteroides Capsule Polysaccharide A

The works explained in the above paragraphs support the idea that the host needs the microbiota to develop a healthy immune system. However, the surface architecture of symbionts that perform these beneficial tasks is not so different from pathogens, because they also have ligands like LPS, peptidoglycans and lipoproteins that are present in pathogens. Ligands from symbiotic bacteria and pathogenic bacteria both are recognized by innate immune receptors such as Toll-like Receptors and can induce an immune response. The fundamental question then becomes how do these symbiotic bacteria control the immune response that they elicit. Dennis Kasper's and Sarkis Mazmanian's groups presented the answer to part of this important question by showing that a very specific molecule on the surface of the bacteria from *Bacteroides fragilis* can induce a regulatory T cell response to induce an anti-inflammatory immune response through its polysaccharide capsule called polysaccharide A (PSA). *B. fragilis* with PSA was able to protect animals from colitis induced by *Helicobacter hepaticus*, a commensal bacterium with pathogenic potential (28). The therapeutic effect of *Bacteroides fragilis* was dependent on the presence of PSA on the surface of the bacteria. Unlike carbohydrates that are classically considered T-cell independent antigens, PSA, a zwitterionic molecule with repeating subunits containing both positive and negative charge, is able to induce T cells by actually being presented on MHC-II by Antigen Presenting Cells (APCs)(29).

In light of the discoveries of immunomodulatory properties of commensal bacteria, especially polysaccharide A from *Bacteroides fragilis*, we wanted to know whether there are other surface structures in commensal bacteria that have immunomodulatory properties. We began our search by focusing on *Bacteroides thetaiotaomicron*, a model human gut symbiont with well-established genetic tools that enable deletion and complementation studies to determine the specific effect of genes encoding surface structures.

During this search, we serendipitously discovered a previously unknown surface protein from *Bacteroides* that is capable of covering the entire cell surface of the bacteria, creating a crystalline lattice surface layer. We found that the formation of this entire proteinaceous capsule is phase-variable, controlled by inversion of a single promoter. Approximately only 0.1% of the population produce this capsule in laboratory culture, but analyzing the fecal metagenome sequence data from the Human Microbiome Project revealed that ~ 8% of the population produce a homologous protein in humans, suggesting its significance *in vivo*. Functional studies revealed that the *BT1927*-expressing

subpopulation is profoundly resistant to complement-mediated killing, due in part to the BT1927-mediated blockade of C3b deposition. Our results indicate that *Bacteroides* is capable of a far greater degree of surface structural variation than previously known, perhaps to cope with the varying environmental conditions in the human intestine.

Chapter 2 : Discovery of a Phase-Variable S-layer in a Human Gut Commensal *B. thetaiotaomicron*

Introduction

Bacteroides phase variation

Bacteroides species are dominant members of the human distal intestinal microbiota (6, 30). The ability of these species to modulate its surface antigenicity is believed to play an important role in their intestinal survival. The multiple capsular polysaccharides of the human colonic microorganism *Bacteroides fragilis* have been extensively characterized. This organism is able to modulate its surface antigenicity by producing at least eight distinct capsular polysaccharides PSA-PSH (PSA, as previously described in Chapter 1, is able to modulate the host immune response through induction of regulatory T cells). The expression of seven of these capsular polysaccharides (except for PSC) is controlled in an on-off manner by a reversible inversion of inverted repeat segments flanking the promoter of each polysaccharide locus (31). The inversion of seven invertible capsule polysaccharide promoters and six other invertible sites distributed throughout the genome are mediated by a global Mpi (multiple promoter invertase), a member of the Ssr (Serine site-specific recombinase) family (32) as well as the local Tsrs (Tyrosine site-specific recombinase) which flip the promoter in their immediate downstream region (33).

The expression of polysaccharides is also controlled at a higher level by the first two genes of each locus, the UpxY and the UpxZ, where x is a-h, depending on the polysaccharide locus. UpxYs are transcriptional antitermination factors that associate with RNA polymerase to prevent premature transcriptional termination (34). UpxZ inhibit the simultaneous expression of more than one polysaccharide by interfering with the activity of UpxY (35). It is believed that this capacity to produce multiple phase-variable capsular polysaccharides with limited concurrent polysaccharide synthesis create populations with diverse surface structure including some that could survive the attack by products made by the host or other members of the microbiota, increasing the organism's probability to sustain colonization inside the intestine (36, 37).

S-layers

The outermost layer of the bacteria reflects the adaptation of the organisms to its surrounding environment. One such outermost layer is the surface layer (S-layer) found in hundreds of species belonging to both Gram-positive and Gram-negative bacteria. S-layers have oblique, square or hexagonal lattice symmetries with one morphological unit consisting of one, two, four, three or six identical protein (or glycoprotein) units with 2-8 nm in diameter identical pores. S-layers self-assemble and cover the entire surface of the bacteria. In Gram-positive bacteria, S-layer is linked to the peptidoglycan layer while in Gram-negative bacteria, S-layers associate with lipopolysaccharides. Although S-layer is a widespread feature of prokaryotic organisms, there existence has not been appreciated because it is often lost during sub-culturing under laboratory conditions. S-layers are some of the most abundant proteins in the bacteria and their biogenesis is thought to consume considerable metabolic resources, reflecting its importance to the organism (38).

Previous studies have shown that various *Bacteroides* species, including *B.*

thetaiotaomicron, have an electron-dense layer–a putative S-layer–outside the outer membrane (39–41). Although most S-layers of *Bacteroides* species are uncharacterized, the S-layer has been described as a virulence factor in *Tannerella forsythia* (previously known as *Bacteroides forsythus*), an organism associated with periodontal disease. Sabet and coworkers showed that S-layers are required for the attachment and invasion of bacteria into epithelial cells, and they suggested that the significant antibody response against *T. forsythia* S-layer may play a role in abscess formation (41).

Rationale for this work

The beginning of my dissertation project started with exploring and finding new surface structures possessed by *Bacteroides* that mediate host-microbe interaction. This chapter will describe our attempt at discovering new surface structures, particularly focusing on the S-layer in *Bacteroides thetaiotaomicron,* which resulted in a serendipitous discovery of a completely novel surface structure in this human-associated gut bacterium.

Results and Discussion

Serendipitous discovery of a cryptic surface layer protein in *Bacteroides*

We began by systematically searching *Bacteroides* genome sequences for gene clusters predicted to encode factors that mediate microbe-host interactions. Three such gene clusters in *Bacteroides thetaiotaomicron* VPI-5482 (hereafter, *Bt*) (*BT1949-1954*, *BT2093-2095*, and *BT4420-4430*) were predicted to contain genes that encode surface layer proteins, which vary widely in composition among microbial taxa but are known to play a role in processes central to microbe-host interaction, including biofilm formation, adhesion, and immune evasion (42). To determine whether these loci specify the production of a surface layer, we constructed strains in which *BT1954*, *BT2095*, or the entire *BT1949-1957* loci were deleted. We then compared cell-surface protein preparations of *Bt* and the mutants by SDS-PAGE, expecting to find cell-surface protein(s) present in the *Bt* preparation but missing from one or more of the mutants. No such proteins were found but, to our surprise, we found reproducibly that one of the mutants, *ΔBT1954*, expressed very high levels of a new cell-surface protein (**Figure 2.1**).

Transmission electron micrographs of the *ΔBT1954* mutant revealed that the electron-dense layer of capsular polysaccharide (43) characteristic of *Bt* was replaced by a novel surface structure that resembles a crystalline surface layer. The hexagonal lattice extends ~500 angstroms beyond the outer membrane, and it appears to cover in a monolayer the entire length of the rod as well as both of its ends (**Figure 2.2**).

As a proteinaceous surface layer has not yet been described in *Bacteroides*, we set out to determine the identity of its constituent protein(s). Cell-free culture fluid from log-phase *ΔBT1954* cells was acidified to precipitate proteins that were secreted or had dissociated from the cell material. We separated the proteins using denaturing polyacrylamide gel electrophoresis, and the most prominent band (apparent molecular weight = ~100 kDa) was excised and subjected to tandem mass spectrometry. Multiple peptide matches confirmed that it is BT1927, a 928 amino acid protein of unknown function (We suspect that the N-terminus is annotated incorrectly in the database, as an earlier start codon would include an additional 12 amino acids that are highly conserved in the homologs of BT1927 (**Figure 2.6**). Residue numbers throughout this dissertation refer to the corrected ORF). Although a distantly related member of human microbiota, *Parabacteroides distasonis* 8503, has been reported to possess a phase-variable S-layer glycoprotein (44), the unambiguous identification of a crystalline S-layer in a *Bacteroides* species is unprecedented.

The expression of *BT1927* is controlled by an invertible promoter

BT1927 resides in a locus adjacent to two site-specific recombinases, *BT1928-1929*, and the 887 bp of intergenic sequence between *BT1927* and *BT1928* contains a 256 bp promoter-containing element flanked by 22 bp inverted repeats (IRs) (**Figure 2.3**). Similar invertible promoter elements are responsible for the phase-variable expression of other surface structures, including capsular polysaccharides (31–33, 44), indicating that the

expression of a new type of capsule might be controlled by a similar mechanism to that of the well-characterized capsular polysaccharides. Consistent with this view, a previously reported analysis of DNA sequencing reads from *Bacteroides fragilis* NCTC 9343 has shown that a promoter of similar architecture that resides adjacent to *BF4087*, a homolog of *BT1927*, exists in both orientations under conditions of laboratory culture, and that the promoter's orientation is controlled by the recombinase Tsr26, a homolog of *BT1928* and *BT1929* (33). In order to determine the orientation of the *BT1927* promoter in the Δ*BT1954* mutant, we amplified the IR element with primers that anneal beyond its 5' and 3' borders and digested the amplicon with the restriction enzyme DrdI, which has a recognition site inside the element that generates asymmetric fragments that are diagnostic of orientation (**Figure 2.4**). We found that in *Bt*, the promoter exists in one orientation (OFF, as described below), but in the *ΔBT1954* mutant, the opposite orientation of the promoter is observed (ON, as described below) (**Figure 2.4**).

As the *BT1927* locus operon is >36 kb away from *BT1954*, we next sought to determine whether *BT1927* is related to *BT1954*. Two lines of evidence suggest that there is no direct relationship between the two proteins: 1) We re-derived the *ΔBT1954* mutant from the merodiploid (single-crossover) intermediate; none of the re-derived mutants harbored the *BT1927* promoter in the ON configuration. 2) We independently constructed mutants in which the expression of *BT1927* was 'locked' on or off by mutating one of the half-sites of its invertible promoter (**Figure 2.5**; hereafter, *BT1927*-ON and *BT1927*-OFF), and neither mutant harbors a polymorphism at the *BT1954* locus. We conclude that (*i*) our initial *ΔBT1954* mutant underwent a rare bottleneck event in which a *BT1927*-expressing variant was inadvertently isolated; (*ii*) *BT1927* is unrelated to *BT1954*, although we cannot rule out the possibility of a high-level regulatory connection between the two loci; and (*iii*) our discovery of *BT1927* was serendipitous. We therefore performed the rest of our experiments with the *BT1927*-ON and *BT1927*-OFF mutants, and *BT1954* was not investigated further.

BT1927 is secreted and localized to the cell surface

We next sought to determine unambiguously that the BT1927 protein product is secreted and localized to the cell surface. The N-terminus of BT1927 harbors a predicted signal peptide, and peptides from trypsin- and Arg-C-digested BT1927 start with T26, suggesting that the protein is cleaved after D25 during the process of secretion. Three bioinformatic findings provided further evidence for the secretion of BT1927: (*i*) the N-terminal 48 aa of BT1927 are highly conserved across its homologs in *Bacteroides* (75-100%) but the remaining 880 aa less so (31-43%), indicating a conserved function for its putative N-terminal signal peptide (**Figure 2.6**). (*ii*) The conserved N-terminal peptide extends longer than a typical signal peptide, suggesting a function beyond that of a typical signal peptide (**Figure 2.7**). (*iii*) BT1927 and its homologs are found adjacent to a predicted outer membrane beta-barrel protein, consistent with BT1927-BT1926 functioning as a two-partner secretion system.

Three lines of experimental evidence suggest that BT1927 is present on the cell surface. First, SDS-PAGE analysis of TCA-precipitated proteins from cell-free culture fluid

reveals a high MW band in the *BT1927*-ON but not *BT1927*-OFF cells; this band corresponds to BT1927, and is the same band that appeared in the Δ*BT1954* mutant (**Figure 2.8**). Second, transmission electron micrographs of the *BT1927*-ON mutant show the same tessellated structure adjacent to the outer membrane as in the Δ*BT1954* mutant, but this structure is absent in the *BT1927*-OFF mutant (**Figure 2.9**). Finally, we constructed mutants in the *BT1927*-ON and *BT1927*-OFF backgrounds in which a FLAG-tag was appended in-frame to the C-terminus of BT1927. Immunocytochemical staining of *BT1927*-ON-FLAG and *BT1927*-OFF-FLAG cells confirmed that BT1927 is present on the surface of the former, but not the latter mutant (**Figure 2.10**). Together, these results suggest that BT1927 is secreted through the inner and outer membranes, forming a novel surface structure adjacent to the outer membrane.

Attempt to generate a Δ*BT1926* mutant

We attempted to generate a **Δ***BT1926* mutant in the *BT1927*-ON background, but the mutant was not isolated after screening 56 colonies, although vector integration into the genome was verified at both integration sites by PCR. Notably, Goodman and coworkers (45) were able to isolate a transposon mutant in *BT1926* in wild-type *Bt*, suggesting that BT1926 can be mutated when BT1927 is not being expressed. In BT1927-expressing cells, BT1926 may be required to avoid the deleterious effects of BT1927 accumulating in the periplasmic space. A similar observation has been made with *Serratia marcescens* Sh1A (a secreted hemolysin) and Sh1B (its partner exporter). When sh1A and sh1B are expressed together in *E. coli*, Sh1A is secreted into the culture medium. However, when sh1B is removed, the hemolysin is not only no longer secreted, but the strain ceases to grow 40 min after IPTG induction (46).

A subpopulation of a wild-type *B. thetaiotaomicron* culture expresses BT1927

Having validated that *BT1927*-ON cells harbor a novel proteinaceous capsule, we next asked what percentage of cells in a laboratory culture of *B. thetaiotaomicron* express BT1927. Because we were able to detect cells with the *BT1927* promoter in the ON orientation using PCR amplification but not the PCR-based restriction digest assay described above, we hypothesized that BT1927-expressing cells occur at a low frequency, requiring us to develop a more sensitive method of detection. Having previously constructed *Bt* mutants in which BT1927 is C-terminally FLAG-tagged in the *BT1927*-ON and *BT1927*-OFF backgrounds, we next constructed a mutant in which BT1927 is C-terminally FLAG-tagged in the parental *Bt* background (hereafter, *BT1927*-FLAG). Cells from all three of the *BT1927*-FLAG strains were labeled with a monoclonal anti-FLAG antibody, and FLAG+ cells were quantified by flow cytometry. As expected, 93.2-97.1% of cells in the *BT1927*-ON-FLAG population had detectable BT1927 expression, while expression in *BT1927*-OFF-FLAG cells was 0.04-0.08%. In a culture of *BT1927*-FLAG, we found reproducibly that 0.15-0.25% of the cells express BT1927, suggesting that cells expressing the proteinaceous capsule form a minority of ~1:1000 cells in a laboratory population of *Bt* (**Figure 2.11**).

The frequency of phase-variants is known to differ from conditions of laboratory culture to growth in an animal host (47, 48). To determine the frequency of this phase-variant *in vivo*, we next analyzed whole-genome-shotgun (WGS) metagenomic sequence data from Human Microbiome Project stool samples in an effort to find a subject colonized predominantly by *B. thetaiotaomicron*. Although we found *BT1927* in 52 out of 86 stool samples (60%), its coverage in those samples was not deep enough to detect both orientations. Instead, we found a subject colonized at a high level by a strain of *Bacteroides fragilis* that harbors a homolog of BT1927. We computationally recruited raw reads from this WGS sample to four loci corresponding to the two orientations of the invertible promoter; an average of 22 reads (~8% of total reads) were recruited to one orientation (presumably ON), while an average of 254 reads (~92% of total reads) are in the opposite orientation (presumably OFF). This finding indicates that the frequency of BT1927 homolog expression may be higher *in vivo* than *in vitro* (**Figure 2.12**).

Our data show that *Bacteroides* can remodel its surface to express a previously unknown proteinaceous capsule, and they suggest that *Bacteroides* populations harbor a greater diversity of subpopulations with distinct capsule types than was previously known. Further exploration of other phase-variable loci might reveal new subpopulations of cells with distinct functions that are important for colonization and microbe-host interactions.

Materials and Methods

Bacterial strains, media and growth conditions

All bacterial strains used in this study are listed in **Table 2.1**. All *Bacteroides thetaiotaomicron* strains were grown at 37 °C in Brain Heart Infusion agar supplemented with 10% horse blood, tryptone-yeast extract glucose (TYG) or *Bacteroides* Minimal Medium (MM) (49, 50) in the anaerobic chamber (COY laboratory products) with a 5% H_2, 20% CO_2 and N_2 balance gas mix. *Escherichia coli* strains were grown aerobically at 37 °C in LB medium supplemented with ampicillin to select for the pExchange-*tdk* plasmid.

Construction of *Bacteroides thetaiotaomicron* mutants

All plasmids and primers are listed in **Tables 2.2**. All mutants were created in the *B. thetaiotaomicron* VPI-5482 Δ*tdk* background, which is referred to in the text as "*Bt*". D*BT1954* was constructed using the counterselectable allele exchange method described by Koropatkin and coworkers (51). Briefly, ~1 kb fragments upstream and downstream of the *BT1954* gene were cloned and fused using primer pairs D*BT1954* Sal-UF/UR and DF/XbaI-DR, respectively, and ligated into the suicide vector pExchange-*tdk* (obtained from Justin Sonnenburg, Stanford University). The resulting vector was electroporated into *Escherichia coli* S17-1 λ *pir* and then conjugated into *Bt.* Single recombinants were selected on BHI-blood agar plates containing 200 mg/mL gentamicin and 25 mg/L erythromycin. Single recombinants were cultured in TYG medium overnight, and then plated onto BHI-blood agar plates containing 200 mg/mL 5-fluoro-2-deoxyuridine (FUdR). Candidate *BT1954* deletions were screened by PCR using the diagnostic primers listed in **Tables 2.2** and confirmed by DNA sequencing to identify isolates that have lost the gene.

BT1927-ON and *BT1927*-OFF mutants were constructed using a strategy adapted from Gunther *et al.* (52). We used the same counter-selectable allele exchange method described above, except that the insert ligated into pExchange-*tdk* was made by fusing three fragments: (*i*) a 1 kb upstream fragment, (*ii*) the promoter region (in ON or OFF orientation) flanked by one native IR sequence and one mutated IR sequence consisting of random DNA sequence, and (*iii*) a 1 kb downstream fragment. The random sequence was generated using a random DNA sequence generator from the UC Riverside Maduro lab website (http://www.faculty.ucr.edu/~mmaduro/random.htm) with the addition of a BglII site to facilitate screening by restriction digest.

The FLAG epitope tag was inserted in-frame at the 3' end of the *BT1927* coding sequence in the *BT1927*-ON and *BT1927*-OFF backgrounds using the same method described above, except that the construct was made by fusing a 1 kb upstream fragment and a 1 kb downstream fragment harboring the FLAG sequence.

Diagnostic digest to determine the orientation of the *BT1927* promoter region

The *BT1927* promoter region was amplified by PCR using primers *BT1927* IR1 and IR2 (**Table 2.2**). The amplicon was cleaned using a QIAGEN PCR Purification Kit, and digested overnight with DrdI. The digested amplicon fragments were separated on a 1% agarose TAE gel and imaged using an Alpha Imager (Protein Simple).

Protein extraction and SDS-PAGE

Bt, Δ*BT1954*, *BT1927*-ON and *BT1927*-OFF were cultured overnight in TYG medium, diluted 1:100 in fresh TYG and grown to log phase the next day (~6.5 hours). The culture supernatant was filtered using a 0.22 mm syringe filter (Millipore) and concentrated using a 10K MWCO Amicon Ultra-15 centrifugal filter (Millipore), and proteins were precipitated by addition of 1 volume of a trichloroacetic acid stock solution (500 g trichloroacetic acid dissolved in 350 mL H_2O) to 4 volumes of supernatant, followed by two cold acetone washes. The precipitate was resuspended in sample buffer and loaded onto a 10% acrylamide gel. Gels were stained with Coomassie Blue for visualization and protein band excision.

Transmission electron microscopy sample preparation and imaging

Bt *culture and initial fixation: Bt* and mutant strains were cultured overnight in TYG medium in the anaerobic chamber at 37 °C. The following day, saturated cultures were diluted 1:50 into 10 mL MM for 15 h at 37 °C in the anaerobic chamber. After 15 h, 7.5 mL 4% glutaraldehyde in MM was mixed with 7.5 mL of the culture and fixed in the anaerobic chamber for 10 min while rocking. The mixture was centrifuged at 3270 x *g* for 10 min and the pellet was resuspended in 2 mL 2.5% glutaraldehyde in 0.1 M sodium cacodylate buffer at pH 7.2 (abbreviated CB). The resulting suspension was aliquoted into microcentrifuge tubes and stored at 4 °C until further processing.

Washing and post-fixation: For the remainder of the sample preparation procedure, all centrifugation steps were performed at ~21,000 x *g* for 1 min. The cell suspension in CB was centrifuged, and cells were resuspended in fresh CB and incubated for 10 min; this wash step was repeated for a total of 3x. After the last wash step, the cells were resuspended in CB supplemented with 1% OsO_4, and 1.6% potassium ferricyanide. Using the PELCO Biowave Pro Microwave Tissue Processor (Ted Pella; abbreviated MW) the cells were fixed by 2 cycles of the following procedure: 2 min heating under vacuum, 2 min vacuum without heating. To remove the OsO_4, the cells were resuspended in CB, heated for 40 s in the MW, centrifuged, and the supernatant was removed. This wash step was repeated a total of 3x.

Uranyl acetate en bloc staining: To remove salts, cells were washed three times by centrifugation, resuspension in deionized (DI) water, and incubation for 10 min at room temperature. Cells were resuspended in 1% uranyl acetate prepared in DI water and stained in the MW using 2 cycles of the following program: 2 min heating under vacuum and 2 min vacuum without heating. Uranyl acetate was removed by resuspending in DI water and heating for 40 s in the MW a total of 3x.

Dehydration and infiltration: Dehydration consisted of the following procedure: centrifugation, resuspension of the cell pellet in 35% ethanol, heating in the MW for 40 s. This process was repeated a total of 2x each with: 35%, 50%, 70%, 80%, 95%, and 100% ethanol, followed by one additional 40 s heating step in 100% ethanol and 40 s of heating in 100% acetone. The cells were pelleted, the acetone was decanted, and then resin was infiltrated (recipe for 50 mg resin: 23.5 mg of Eponate 12 resin, 12.5 mg of dodecenyl

succinic anhydride (DDSA), 14 mg of nadic methyl anhydride (NMA), and 0.75 mL of benzyldimethylamine (BDMA)) at a ratio of 3:1 acetone: resin. This mixture was subjected to 2 cycles of 3 min heating under vacuum in the MW. The same procedure was repeated with a 1:1 and then a 1:3 mixture of acetone: resin. Finally, cells were resuspended in pure resin, heated under vacuum in the MW for 3 min, and then centrifuged; this final procedure was repeated a total of 3x. Cells were placed in a beam capsule and heated in a 55 °C oven for 2 d.

Ultrathinsectioning and imaging: The resin-embedded cells were ultrathin-sectioned using a diamond knife. Sectioned samples were inserted into a PELCO grid staining system. Samples were stained in 2% methanolic uranyl acetate (2% uranyl acetate dissolved in 70% methanol/H_2O) for 5 min at room temperature, washed 5x in DI water, and then stained in Reynolds lead citrate (recipe for 50 mL: 1.33 g lead nitrate and 1.76 g of sodium citrate dihydrate were dissolved in 30 mL DI H_2O, to which 8 mL of 1 N NaOH was added, followed by 10 mL of DI H_2O) for 5 min at room temperature. 10 more washes were performed with DI water, and the sample was dried with a Kimwipe and imaged on the FEI Tecnai 12 transmission electron microscope. The images were cropped and their size was compressed using Adobe Photoshop. ImageJ was used to add the scale bar.

Immunofluorescent labeling and microscopy

Immunofluorescent labeling was performed according to the protocol described by Moyes (53). Briefly, bacteria were cultured in TYG medium overnight in the anaerobic chamber at 37 °C. Saturated cultures were diluted 1:50 into 10 mL MM and incubated for 15 h at 37 °C in the anaerobic chamber. Following incubation, cultures were centrifuged at 3720 x g for 10 minutes, washed with Phosphate buffered saline (PBS, 137 mM NaCl, 2.7 mM KCl, 10 mM Na_2HPO_4, 1.8 mM KH_2PO_4) and resuspended to approximately 10^7-10^8 cfu/mL. A smear was prepared by spreading 20 ml of the resuspended cells using a sterile loop on a clean microscope slide, air-dried in the fume hood, submerged in 95% EtOH and heat-fixed by incubating in the 55°C oven for 10 min. Slides were incubated with an anti-FLAG antibody conjugated to Alexa fluor 647 (Cell Signaling, diluted 1:100 in PBS) for 30 min at 37 °C, rinsed, and incubated in PBS for 30 min at room temperature. Labeled cells were counterstained with SYTO BC Bacteria Stain (Molecular Probes). Images were acquired using a 100x objective on a 6D High Throughput Microscope at the UCSF Nikon Imaging Center. The images were cropped and their size was compressed using Adobe Photoshop. ImageJ was used to add the scale bar.

Flow cytometry to quantify *BT1927*-expressing cells

Bt and mutant strains were grown in TYG medium overnight diluted 1:100 in fresh TYG medium and grown to late log phase (~6.5 h). 1 mL of the culture was centrifuged for 2 min in a microcentrifuge at 6000 x *g*, washed twice with PBS, and resuspended to approximately 50 x 10^6 cells/mL in Bacteria Staining Buffer (BSB, 1% bovine serum albumin, 0.025% sodium azide in PBS). In a V-bottom 96-well cell culture plate (Corning), 25 mL of the resuspended bacteria were mixed with 25 mL anti-FLAG Alexa fluor 647 conjugated antibody (Cell Signaling, diluted 1:25 in BSB) and incubated for 1 h at 37 °C. The

96-well plates were centrifuged at 3273 x *g* on a Beckman tabletop centrifuge for 4 min to pellet the cells and washed twice with 150 mL BSB. Cells were counterstained with SYTO BC Bacteria Stain (Molecular Probes) and analyzed on a LSRII flow cytometer. In order to minimize carry-over of cells, 3 blank samples of PBS were included between samples. FSC and SSC were set to logarithmic scale. Two populations (top and bottom) were visible on the FSC and SSC plot, where the bottom population was present even in sterile H_2O, bleach and PBS without any bacteria and the top population was present only in samples with bacteria. Therefore, a gate was set to exclude the bottom population and 500,000 events were collected on the top population. After data acquisition, the top *Bt* population was visualized on an APC vs. FITC plot and further separated by quadrants, which were set using the unstained sample. Spectral overlap was calculated from single-stained controls. All post-acquisition analyses and compensations were performed using FlowJo (Tree Star).

Computational analysis of *BT1927* and its homologs in stool samples sequenced by the Human Microbiome Project

The protein sequence of BT1927 was used as a query sequence for BLASTp searches against a translated database of assembled contigs from each of the first-visit stool samples sequenced by HMP (n = 86, available at HMP DACC). BT1927 was deemed "present" in a sample when a protein sequence was detected as a hit, with an expectation value < 1.0 e-50. The relatively low coverage of *Bt* in these samples (~20-30 X, as determined by coverage calculation for the BT1927 inverted repeat region in a subset of these samples) prevented us from determining the orientation of the *BT1927* promoter region. We then performed a similar BLAST search to identify BT1927 homologs from other *Bacteroides* sp. with high depth of coverage in the HMP samples. One sample, SRS016267, harbored a *B. fragilis* BT1927 homolog at 477x coverage. Quality-filtered and trimmed reads of SRS016267 were obtained from HMP DACC and used to determine the frequency of both orientations of this gene's promoter. Briefly, we divided the inverted repeat/promoter region of the BT1927 homolog into four sequence blocks of 100 bp, where each block consists of 18 bp of each of the inverted repeats flanked by 41 bp on each side to determine its orientation. Two blocks corresponded to the upstream and downstream inverted repeat sequences of orientation 1, and the other two blocks corresponded to the upstream and downstream inverted repeat sequences of orientation 2. SRS016267 reads matching these blocks were identified using BLASTn with a cutoff expectation value of 1.0 e-31, which we determined to be necessary to unequivocally assign the orientation. To further confirm their orientation, these reads were mapped to the corresponding sequence block using Geneious with the following parameters (minimum percent identity at overlap: 90%, and maximum percentage of mismatch per read: 20%), and the average coverage of each block was calculated only from the mapped reads.

Figures and Tables

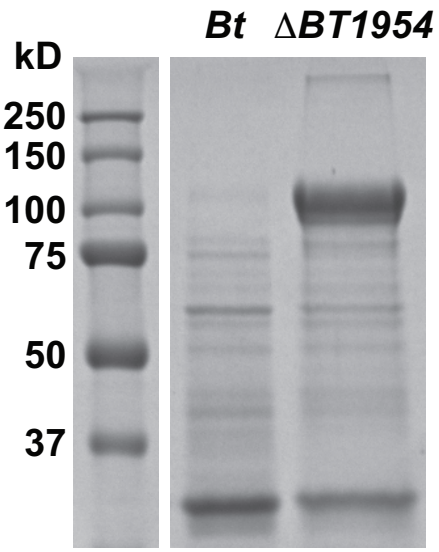

Figure 2.1 An abundant high molecular weight surface protein in *B. thetaiotaomciron.* Proteins were precipitated from filtered culture supernatants of *Bt* with trichloroacetic acid and subjected to SDS-PAGE. The Δ*BT1954* culture supernatant harbors an abundant, high molecular weight band that is absent in *Bt*.

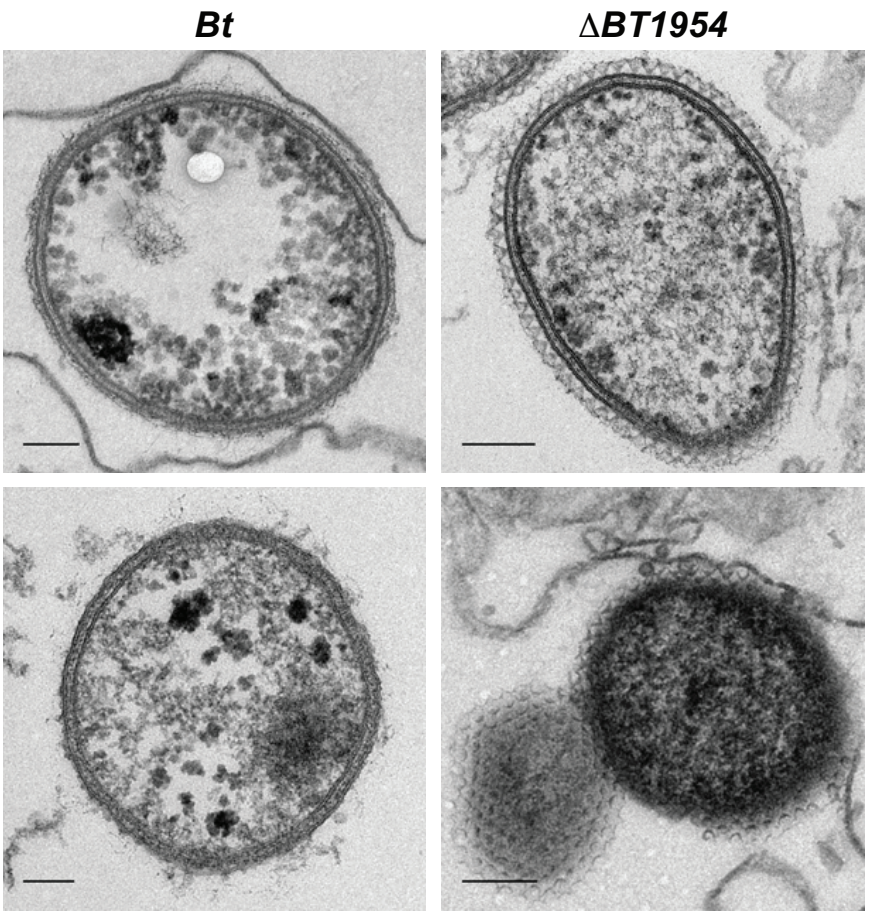

Figure 2.2 Transmission Electron Microscopy of *B. thetaiotaomicron.* *Bt* cells were fixed, ultrathin-sectioned, negative-stained and imaged through a transmission electron microscope. The Δ*BT1954* mutant (upper right, lower right) harbors a tessellated surface layer adjacent to the outer membrane, which is absent in the parental strain (upper left, lower left). Each scale bar represents 100 nm.

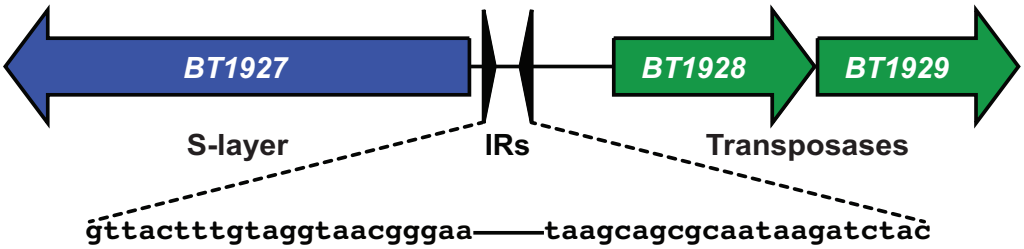

Figure 2.3 Schematic of the *BT1927-BT1929* locus. Schematic showing inverted repeat elements flanking the predicted *BT1927* promoter.

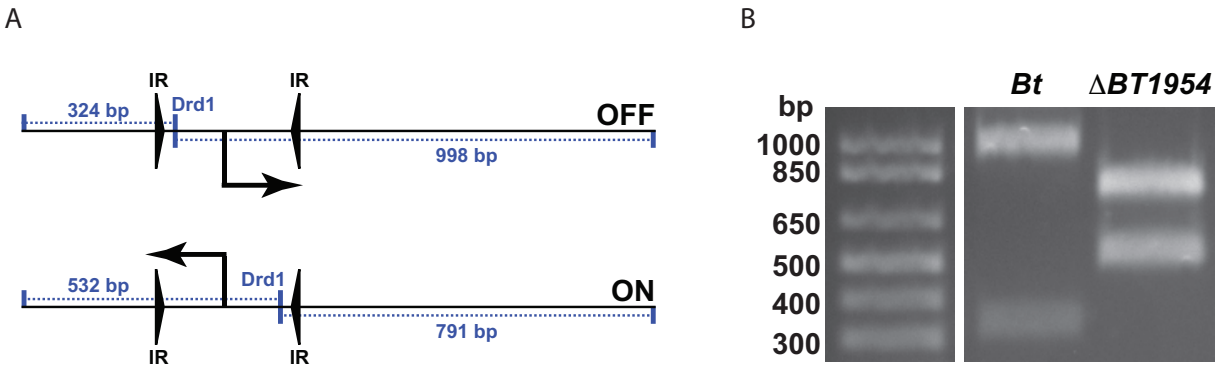

Figure 2.4 *BT1927* promoter orientation assay. On the left is the schematic for the promoter orientation assay. On the right is the result of the DrdI-digested PCR products were separated by agarose gel electrophoresis. The inverted repeat element harboring the predicted *BT1927* promoter is in the opposite orientation in the parental strain and the D*BT1954* mutant.

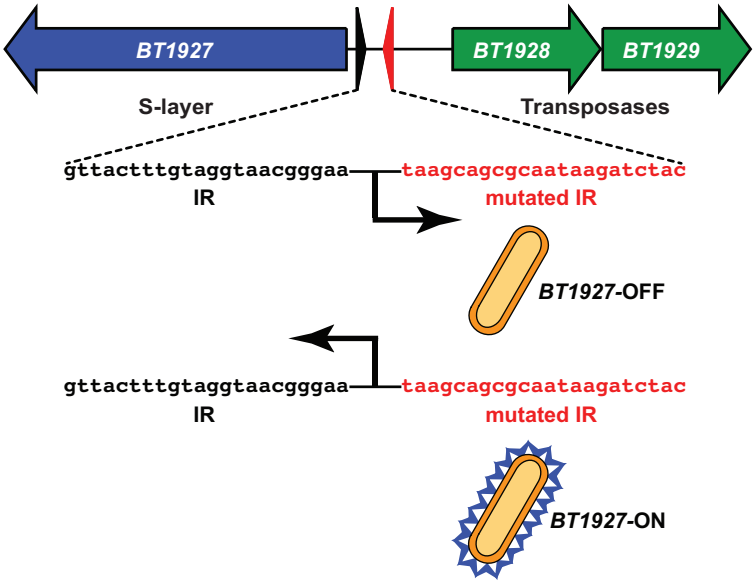

Figure 2.5 Construction and characterization of *BT1927*-ON and *BT1927*-OFF mutants. One half-site of the inverted repeat surrounding the predicted *BT1927* promoter was mutated to create strains in which this element could no longer flip, 'locking' the expression of *BT1927* on (*BT1927*-ON) or off (*BT1927*-OFF).

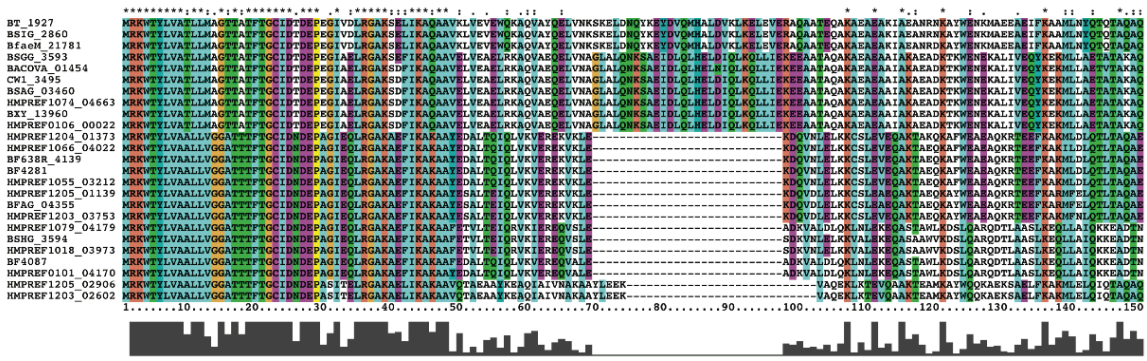

Figure 2.6 BT1927 amino acid sequence alignment with its homologs. The corrected amino acid sequence of BT1927 was aligned with BT1927 homologs in *Bacteroides* species using ClustalX. Note that the first ~50 amino acids is highly conserved.

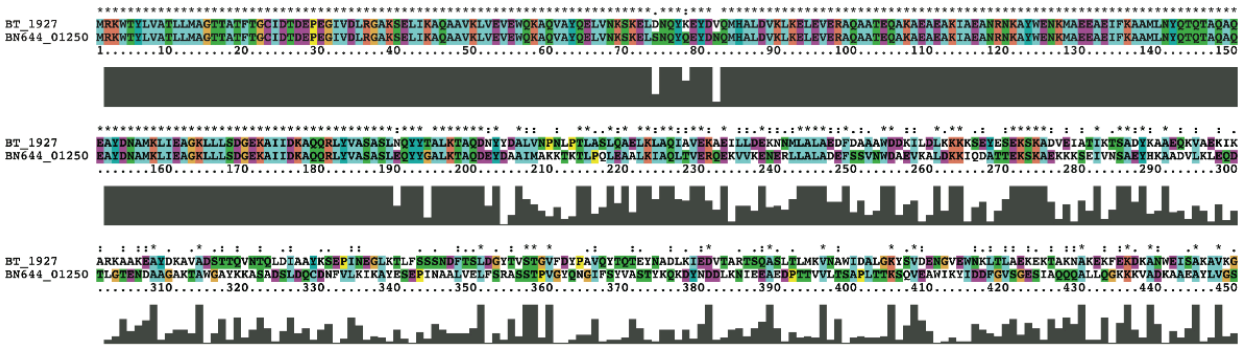

Figure 2.7 BT1927 sequence alignment with *B. thetaiotaomicron* CAG:40. The BT1927 amino acid sequence was aligned with a *BT1927* homolog in *B. thetaiotaomicron* CAG:40, which showed almost a complete match for the first ~200 amino acids.

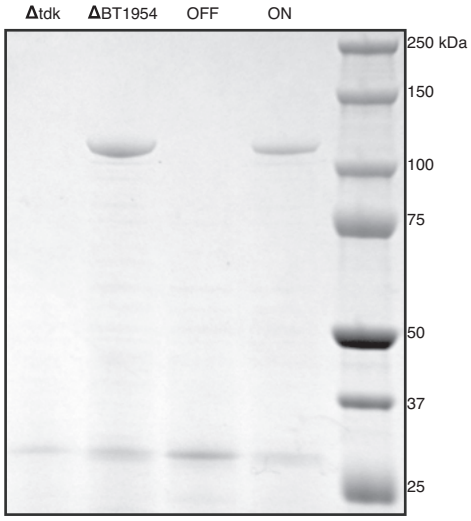

Figure 2.8 Analysis of BT1927 expression in *BT1927*-ON and *BT1927*-OFF by SDS-PAGE. Surface proteins were isolated from culture supernatants of the *BT1927*-ON and *BT1927*-OFF mutants by TCA precipitation, and separated and visualized by SDS-PAGE.

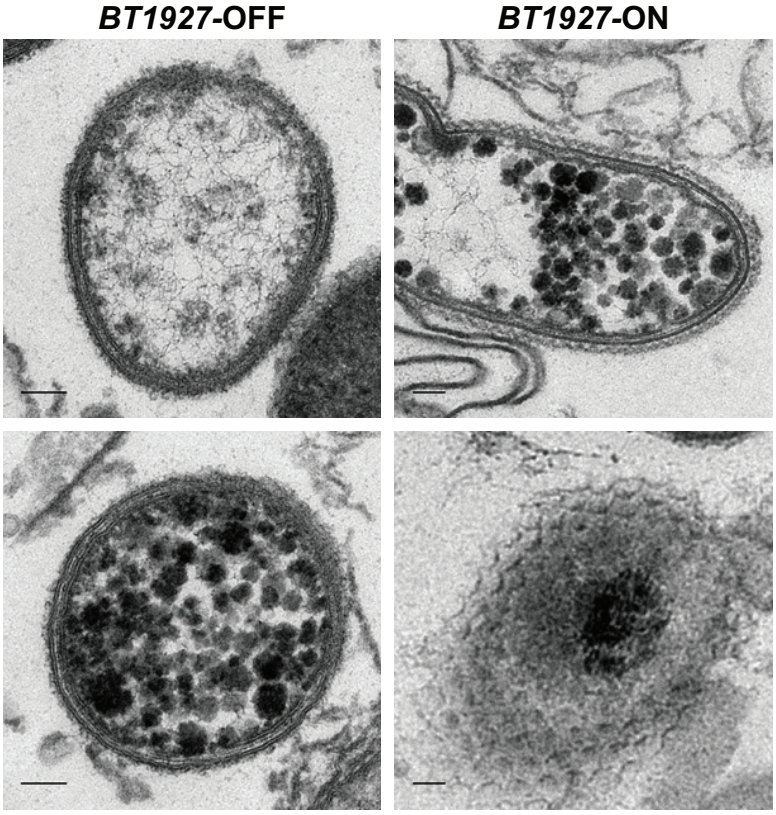

Figure 2.9 TEM of the *BT1927*-ON and *BT1927*-OFF mutants. Cells of the *BT1927*-OFF (upper left, lower left) and *BT1927*-ON (upper right, lower right) mutants were prepared as described in the Figure 2.2 and visualized by transmission electron microscopy, confirming the presence of the same surface structure in *BT1927*-ON that was observed in the Δ*BT1954* mutant. Each scale bar represents 100 nm.

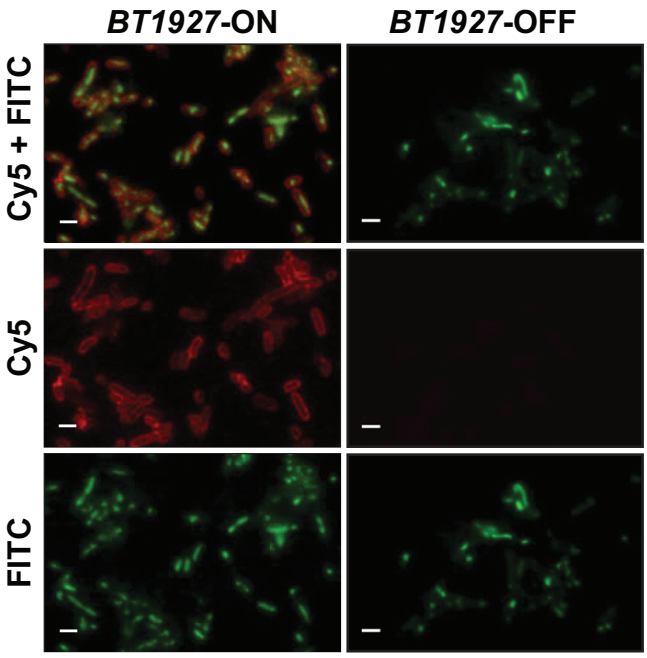

Figure 2.10 Immunofluorescent microscopy of *BT1927*-ON-FLAG and *BT1927*-OFF-FLAG mutants. *BT1927*-ON-FLAG and *BT1927*-OFF-FLAG cells were washed, stained with an anti-FLAG antibody conjugated to Alexa 647 and the DNA stain SYTO BC, and visualized by fluorescence microscopy. Cell surface staining in the *BT1927*-ON-FLAG mutant but not the *BT1927*-OFF-FLAG mutant is consistent with localization of BT1927 to the cell surface. Each scale bar represents 2 mm.

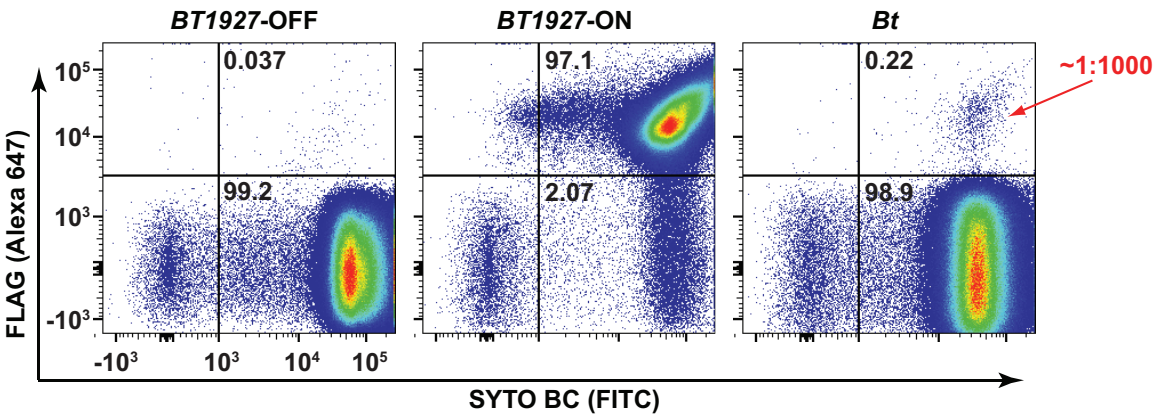

Figure 2.11 *BT1927* is expressed in a subpopulation of *B. thetaiotaomicron.* *BT1927*-ON-FLAG, *BT1927*-OFF-FLAG, and *BT1927*-FLAG cells were washed, stained as described above, and analyzed by flow cytometry to measure the frequency of BT1927-expressing cells in each culture. As expected, the BT1927-expressing population (upper right quadrant) dominates the *BT1927*-ON culture and is nearly absent in the *BT1927*-OFF culture. The *BT1927*-FLAG culture reproducibly showed a BT1927-expressing subpopulation that represents ~1:1000 cells in the population.

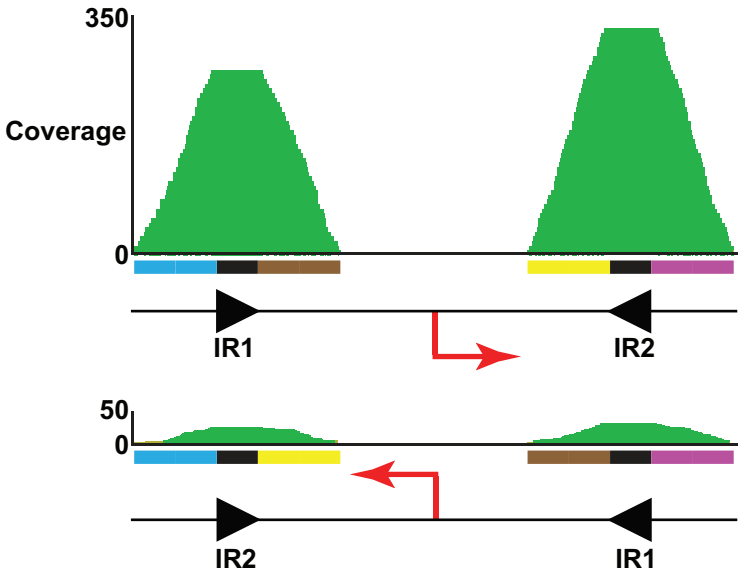

Figure 2.12 Metagenome data from the HMP project suggest *BT1927* homolog is expressed at a higher frequency. The frequency of the two promoter orientations of a *BT1927* homolog in a whole-genome shotgun metagenomic sequence sample from the NIH Human Microbiome Project was measured by recruiting raw sequence reads to each promoter orientation. 92% of the reads are recruited to one orientation (presumably OFF), and the remaining 8% of the reads are recruited to the opposite orientation (presumably ON), suggesting that the BT1927-expressing cells might exist at a higher frequency *in vivo* than *in vitro*.

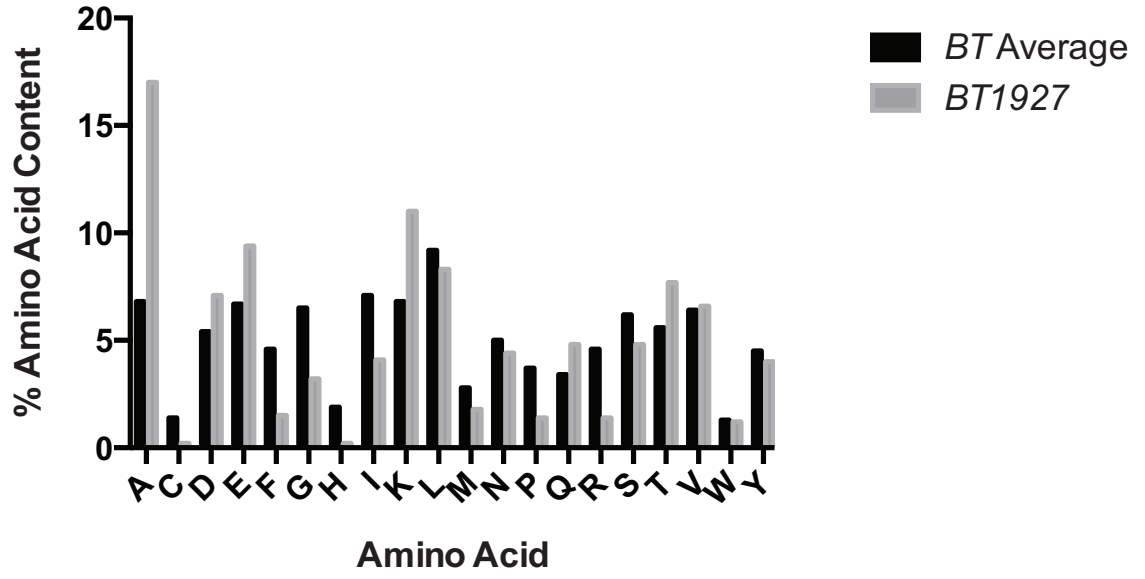

Figure 2.13 The amino acid sequence composition of BT1927. The amino acid composition of BT1927was compared to the average % amino acid composition of *Bt* proteins.

Strain	Plasmid	Source
Escherichia coli S17-1λ pir	NA	Gift from Dr. Justin Sonnenburg, Stanford University
Escherichia coli S17-1λ pir	pExchange-*tdk*	Gift from Dr. Justin Sonnenburg, Stanford University
Escherichia coli S17-1λ pir	*BT1927* C-term FLAG in pExchange-*tdk*	This work
Escherichia coli S17-1λ pir	*ΔBT1954* in pExchange-*tdk*	This work
Escherichia coli S17-1λ pir	*BT1927* promoter locked ON in pExchange-*tdk*	This work
Escherichia coli S17-1λ pir	*BT1927* promoter locked OFF in pExchange-*tdk*	This work
B.thetaiotaomicron VPI-5482 Δtdk	NA	Gift from Dr. Justin Sonnenburg, Stanford University
B.thetaiotaomicron VPI-5482 Δtdk FLAG	NA	This work
B.thetaiotaomicron VPI-5482 Δtdk ΔBT1954	NA	This work
B.thetaiotaomicron VPI-5482 Δtdk BT1927 promoter locked ON	NA	This work
B.thetaiotaomicron VPI-5482 Δtdk BT1927 promoter locked OFF	NA	This work
B.thetaiotaomicron VPI-5482 Δtdk BT1927 promoter locked ON FLAG	NA	This work
B.thetaiotaomicron VPI-5482 Δtdk BT1927 promoter locked OFF FLAG	NA	This work

Table 2.1 List of bacterial strains used in this study

Use	Name	Sequence
ΔBT1954 Primers	SalI-UF	GCG GTC GAC AAT GAC GTG CTT CAG GCT TT
	UR	CAT TAC GGG TAC TCT GGT TAA G
	DF	CTT AAC CAG AGT ACC CGT AAT GTA ACG AGG AAG GAG GAC AAA AAT G
	XbaI-DR	GCG TCT AGA GCC ATT TCT CTG AAG GAG CA
	Diagnostic F	GGG GTC TTG TCC GTA AAC AA
	Diagnostic R	AGA AAC GGA ACC GGA AAA CT
BT1927 Locked mutant primers	SalI-UF (A)	GCG GTC GAC TTA GCA GCT TTA CGC GCT TT
	UR (B)	TAA GCA GCG CAA TAA GAT CTA CGG AAA GAC AGA CCA CCA AGA TG
	OFF-DF (C)	GTA GAT CTT ATT GCG CTG CTT AAG CGT ACT TTT CCA CCC CG
	ON-DF (D)	GTA GAT CTT ATT GCG CTG CTT AGA AAA GAC GCT GCA AAT ATG
	XbaI-DR (E)	GCG TCT AGA TTT CAA GAT GGC CAG GTA GC
	Diagnostic F	TTC AAT CCT TCA TTA ATA GGT TCA GA
	Diagnostic R	ATC ACG CAG CTT CTC GAA AT
BT1927 C-terminus FLAG tag primers	SalI-UF Short	GCG GTC GAC AGG CTA AAG CTG CAT TGG TT
	UR	TTT GTC ATC GTC GTC CTT GTA GTC CAT TAG CAA GGT TGC GAC CAA AT
	STOP-FLAG-BT1927R	TTA TTT GTC ATC GTC GTC CTT GTA GTC CTT ACT CAA GGT TTC CAA TAC G
	FLAG-STOP-BT1927DF	GAC TAC AAG GAC GAC GAT GAC AAA TAA TTT CTT AAT CAC GTA AAA GTA AC
	XbaI-DR	GCG TCT AGA CCA ATG AAA AAG GGC AAA AG
	Diagnostic F	GCA TTG ACT CCT GCT GAA CA
	Diagnostic R1	TTA TTT GTC ATC GTC GTC CTT GTA GTC
	Diagnostic R2	TTT GTC GTG TCT GCA AAA GC
BT1927 Orientation Assay	BT1927 IR 1	AAG CTA CTT GCG CTT TTT GC
	BT1927 IR 2	GGA ATT GAA GGC CGA GTG TA

Table 2.2 List of primers and their sequences used in this study. Restriction sites are underlined.

Chapter 3 : Function of the S-layer in *B. thetaiotaomicron*

Introduction

Functions of the S-layers are diverse, but their immunomodulatory effect is well known

Despite providing an apparently conserved 2D crystalline array, previous literatures report that the function of the S-layer proteins can be extremely diverse (38, 42). The most well studied are the functions of the S-layer possessed by commensals and pathogens. S-layer is the outermost layer that can directly interact with the host immune system, contributing to virulence of pathogens.

Lactobacillus crispatus is a member of the human and chicken gut microbiome that possesses an S-layer protein CsbA (or called SlpB). This S-layer protein has an amino-terminal domain that binds to type I and IV collagen and a carboxy-terminal domain that binds to the bacterial cell wall. The ability for CbsA to bind to collagen is thought to have an important role in colonization of the gut (54).

In *Clostridium difficile*, the etiologic agent of the antibiotic-associated diarrhea, the immune response of the Surface Layer Protein (SLP) has been well documented. *C. difficile* has a high molecular weight SLP and a low molecular weight SLP, both of which are produced by the precursor protein SlpA. Ausiello and coworkers have shown that purified *C. difficile* SLP can induce resting monocytes to secrete cytokines IL-12, TNFα, IL-10 and induce maturation of monocyte-derived dendritic cells (55). Others have also found that the activation of the dendritic cells were dependent on the presence of the Toll-like receptor 4. The authors suggest that TLR4 has an important role in *C. difficile* clearance since infection of TLR4-knockout mice resulted in more severe symptom than in wildtype mice. Interestingly, both the HMW and LMW SLPs of *C. difficile* were required for the activation of dendritic cells, which suggests that either a complex formed by the two proteins is recognized by TLR4, or that one of the SLPs is the actual ligand but it needs the other in context (56). Binding studies have also shown that SLP also play an important role in adhesion to the intestinal mucosa (57). *C. difficile* also has a phase-variable S-layer protein cell wall protein V (CwpV) which its expression is controlled in a similar manner to *BT1927* (58), and shows auto-aggregation when expressed (59).

Campylobacter fetus is another pathogen, which can cause spontaneous abortion, infertility and bacteremia in cattle, sheep and in immunocompromised humans. *C. fetus* S-layer has been shown to confer resistance to complement-mediated killing as well as phagocytosis by macrophages in non-immune serum by preventing the binding of C3b to *C. fetus* cell surface (60). Although *C. fetus* is susceptible to complement independent killing, utilizing the opsonic antibodies directed against the S-layer, *C. fetus* also evolved mechanisms to avoid this antibody-mediated killing by high-frequency antigenic variation of the surface layer proteins. This involves complex DNA recombination of the 626 bp homologous 5' end of the SLP encoding sap genes, moving the promoter upstream of another sap gene (60). The *C. fetus* genome contains up to eight sap genes, but usually only one sap gene is expressed in lab culture, although bacterial subpopulations that express other Sap proteins can be identified. Antigenic variation occurs during *C. fetus* infection in humans as definitively shown by studies analyzing strains that were isolated during the early and late stages of infection from individuals with *C. fetus* infections. In three of the

four patients studied, the strain had undergone a switch in the major S-layer protein that is expressed (61).

Tannerella forsythia (previously known as *Bacteroides forsythus*) is a Gram-negative anaerobic bacterium that is associated with severe forms of periodontal disease. *T. forsythia* concomitantly express two high molecular weight proteins tfsA and tfsB that constitute the S-layer (41). Both proteins are post-translationally modified with motifs including a pseudaminic acid Pse5Am7Gc, a sialic acid derivative. The glycosylation of the S-layer protein seems to be necessary for regulating biofilm formation. TfsA and tfsB also seems to play a role in adhesion and invasion during infection, as shown by studies using human gingival epithelial cells (Ca9-22 cells) and mouth epidermal carcinoma cells (KB cells)(62).

In *Aeromonas salmonicida*, a fish pathogen, the surface A-layer (composed of A-proteins) confers resistance against complement-mediated lysis in the presence and absence of specific antibodies in vitro (63, 64). It has also been shown that A-layer bound rabbit IgG and human IgM with high affinity. They observed that IgG bound only weakly to purified A-proteins, but regained its binding activity when they were reassembled (65). Later, it was shown that *A. salmonicida* S-layer is involved in host cell invasion and lysis, which may constitute survival strategy in vivo (66).

Rationale of this work

Having the previous functional studies of S-layers in mind, we turned to the question of whether the *B. thetaiotaomicron* subpopulation expressing a proteinaceous capsule is functionally distinct from the majority of cells expressing a conventional polysaccharide capsule. To begin addressing this question, we subjected the *BT1927*-ON and *BT1927*-OFF mutants to a set of assays relevant to colonization and growth in the mammalian gut: resistance to complement mediated lysis, recognition by IgA, tropism in the small and large intestine, sensitivity to antimicrobial peptides and activation of TLR2 and TLR4.

Results and Discussion

BT1927-ON cells are resistant to complement-mediated killing

Complement is a component of the innate immune system consisting of circulating and cell-surface-bound proteins that perform a series of extracellular proteolysis. There are three main ways in which the complement system is activated: the classical pathway, the alternative pathway, or the mannose-binding lectin pathway. All pathways converge at the central cleavage of C3 and the generation of its active fragments C3a, an anaphylatoxin, and C3b, an opsonin. Opsonization of C3b covalently bound to the bacterial surface promotes cell clearance by phagocytosis, amplifies complement activation by formation of C3 convertase, a step required for all pathways to form the membrane attack complex (MAC). Since previous reports have documented that S-layers from pathogenic bacteria such as *Campylobacter fetus* and *Aeromonas salmonicida* provide resistance to complement mediated lysis, we simply asked the question, are *BT1927-ON* less susceptible to complement-mediated lysis? In order to answer this question, we simply incubated *BT1927-ON* cells or *BT1927*-OFF cells with serum or heat-inactivated serum, plated the mixture onto agar plates, and counted the number of cells that survived. We found that *BT1927*-ON cells are highly resistant to complement-mediated killing. When incubated with 20% human serum for 60 min, 48.18 ± 12% of the *BT1927*-ON cells survived as compared to just 0.97 ± 0.18% of the *BT1927*-OFF cells (**Figure 3.1**); similar results were obtained by varying serum sources (human, rabbit) and concentrations.

Bt activates the alternative complement pathway

In order to determine which of the three complement activation pathways – classical (antibody-dependent), alternative (antibody-independent), or mannose-binding lectin – were responsible for killing *Bt*, we incubated *Bt* in 20% human serum in the presence of EDTA or Mg-EGTA, which chelate magnesium (required for the alternative pathway) and calcium (required for the classical pathway), respectively. We then prepared lysed bacterial cells and performed a western blot to look for the presence of C3b, a fragment of complement protein C3 that attaches to the surface of bacterial cells in amide or ester linkage via a thioester bond that forms during its proteolytic cleavage from parental C3. The western blot revealed a high-intensity band of ~250 kDa that we presume to be a C3b-bacterial surface protein conjugate, demonstrating as expected that C3b is deposited on the surface of *Bt.* This band was present in preparations incubated in the presence of Mg-EGTA but not EDTA, indicating that the alternative pathway is responsible for *Bacteroides*-directed complement activation (**Figure 3.2**), consistent with previous reports on related *Bacteroides* species (67–69).

C3b deposition is interfered in *BT1927-ON*

To explore the molecular underpinnings of complement resistance in the BT1927-expressing subpopulation, we turned to the question of what step in the complement cascade is blocked by BT1927-expressing cells. We tested the integrity of C3b deposition, a key step in the complement pathway that is known to be subverted by bacterial pathogens.

We incubated the *BT1927*-ON and *BT1927*-OFF strains with human serum, labeled cells with FITC-conjugated anti-human C3 $F(ab')_2$ and performed flow cytometry to assess the level of C3 fragments associated with bacterial cells. As shown in **Figure 3.3 and Figure 3.4**, C3 or its fragments associate with *BT1927*-ON cells with delayed kinetics and at lower efficiency relative to *BT1927*-OFF cells. These results suggest that BT1927-mediated blockade of C3b deposition is at least partly responsible for the resistance of the BT1927-expressing subpopulation to complement-mediated killing.

Complement in the gut

Previous work has shown that surface layer proteins from pathogenic bacteria such as *Campylobacter fetus* confer resistance to complement-mediated lysis (70, 71), one of several strategies used by pathogens to evade the complement system (72). However, *B. thetaiotaomicron* is a commensal, not a pathogen or pathobiont, and is therefore unlikely to encounter the complement system in serum. Although little is known about the interaction between complement and the gut microbiota, two lines of evidence suggest the plausibility of such an interaction. First, complement components are known to be deposited into the lumen and epithelial surface of the murine and human GI tract (73, 74): C3b/iC3b and MAC have been found in the gut lumen of inflammatory bowel disease patients (75, 76), C3 is deposited in the colonic epithelium of mice infected with *Citrobacter rodentium* (77), and C3 and C4 are secreted into the healthy human colonic mucosa (78, 79). *B. thetaiotaomicron* and other gut commensals may therefore encounter components of the complement system under normal conditions of colonization.

Second, recent studies suggest that the C5a receptor regulates the composition of the intestinal and cutaneous microbiota, and helps to maintain a dysbiosis of the oral cavity driven by *Porphyromonas gingivalis* (80–82). Although a specific interaction between a member of the gut microbiota and the complement system has not yet been described, the fact that a conserved *Bacteroides* surface protein mediates complement resistance raises the possibility that complement plays a broader role than previously recognized in modulating the composition and function of the commensal gut microbiota.

Our data show that *Bacteroides* can remodel its surface to express a previously unknown proteinaceous capsule, and they suggest that *Bacteroides* harbor a greater diversity of subpopulations with distinct capsule types than was previously known. They also reveal that a conserved protein in a common gut commensal mediates resistance to complement, raising the intriguing possibility that the BT1927-expressing subpopulation might be able to colonize a different niche in the mammalian intestine that has greater access to complement. Further exploration of other phase-variable loci might reveal new subpopulations of cells with distinct functions that are important for colonization and microbe-host interactions.

***BT1927*-ON and *BT1927*-OFF activate the TLR2 pathway at similar levels**

We next asked whether the structural difference in *BT1927-ON* and *BT1927-OFF* mutants induced a difference in their ability to activate innate immune receptors, such as Toll-like receptors. Toll-like receptors are evolutionarily conserved and recognize microbial ligands of highly conserved structural motifs, known as pathogen-associated

molecular patterns (PAMPS). Previous studies have shown that *Bacteroides thetaiotaomicron* and *Bacteroides fragilis* can signal through TLR2 and TLR4 (83–86).

When we incubated whole cells of *BT1927*-ON or *BT1927*-OFF mutants to bone marrow derived macrophages and measured the amount of cytokine TNFα secreted from them, we found that wildtype and TLR2 only macrophages both secreted a similar amount of TNFα, while TLR4 only macrophages had significantly less TNFα secretion suggesting that *B. thetaiotaomicron* mainly stimulates TNFα secretion through the TLR2 pathway as previously described in *B. fragilis* (83, 85). Surprisingly, although the two mutants have completely different capsules, they both stimulated TNFα secretion through TLR2 at the same level, suggesting the two mutants have similar ability to activate these innate immune receptors, at least in the conditions we used (**Figure 3.5**).

BT1927-ON is slightly more resistant to antimicrobial peptide LL-37

Next, we asked whether *BT1927*-ON and *BT1927*-OFF populations are differentially susceptible to antimicrobial peptides that *Bt* could encounter in the mammalian gut. Antimicrobial peptides are basic peptides 20-40 amino acid in length that is secreted by the host with potent activities against Gram-negative and Gram-positive bacteria. Some prominent ones in the gastrointestinal tract are those in the family of defensins, cathelicidins, and C-type lectins. In order to determine whether *BT1927*-ON and *BT1927*-OFF mutants have a differential susceptibility to antimicrobial peptide, we took a growth curve of the *BT1927*-ON and *BT1927*-OFF mutants in the presence of various physiologically relevant concentrations of the active form of cathelicidin LL-37 (0-20 μg/mL). We found that in the presence of LL-37, *BT1927*-ON and *BT1927*-OFF mutants are both susceptible to LL-37 at 5 μg/mL. There is a slight difference in susceptibility at 1 μg/mL, where *BT1927*-ON shows a slight advantage in growth. Although this could be an advantage for *Bt* expressing *BT1927* during colonization in the mammalian gut, we did not proceed to any further experiments with this observation (**Figure 3.6**).

BT1927-ON and OFF colonize GF mice at similar levels

Next, we asked the whether we could find a differential phenotype between *BT1927*-ON and *BT1927*-OFF mutants *in vivo*. In order to study the function of the S-layer in an *in vivo* setting, we asked our collaborators at Stanford University to send us feces, serum and colon tissues of Germ Free (GF) mice that were colonized with exclusively *BT1927*-ON or *BT1927*-OFF. Using these samples, we analyzed whether there were any differences in colonization levels, bacteria specific antibody levels and tropism in the small and large intestine. We first verified that *BT1927*-ON and *BT1927*-OFF colonize the GF mouse gut at the same level by performing quantitative PCR on the genomic DNA extracted from fecal samples sent to us which were isolated from monoassociated mice. Using two sets of *Bt* specific 16S primers, we confirmed that there were no significant differences in colonization levels between *BT1927*-ON and *BT1927*-OFF from calculated Cp values (**Figure 3.7**). We therefore concluded that the two strains have no difference in the ability to colonize the mouse gut, and proceeded with further assays.

Antibodies from *BT1927*-ON and *BT1927*-OFF monoassociated mice bind to both strains at similar affinity and are induced at similar levels

After verifying that the *BT1927*-ON and *BT1927*-OFF colonized GF mice to similar levels, we next asked whether the two mutants differed in the way they induced an antibody response. Secretory IgA is the main antibody of mucous membranes thought to play an important role in compartmentalizing the microbiota (1, 87, 88) but recently, there has been interest in the role of other antibody isotypes in compartmentalizing the microbiota, such as IgG1 and IgG3 (personal communication with Greg Barton and Meghan Koch). Therefore, we analyzed the specific induction of isotypes IgA, IgG1, and IgG3 by *BT1927*-ON and *BT1927*-OFF. Briefly, we isolated bacteria from feces taken from *BT1927*-ON or *BT1927*-OFF monoassociated mice (or GF mouse as a control) and labeled them with sera taken from *BT1927*-ON or *BT1927*-OFF monoassociated mice at Day 7 and Day 14 post-inoculation. Then we stained the labeled bacteria with anti-IgA, anti-IgG1 and anti-IgG3 antibody conjugated to RPE, APC and Biotin, respectively. Secondary antibodies conjugated to Streptavidin-PECy7 were further added to detect each of the antibody isotype levels via flow cytometry.

First, we analyzed whether the antibody response generated by *BT1927*-ON and *BT1927*-OFF monoassociated mice were specific to the corresponding strain in which the mouse was colonized. In other words, we wanted to know whether antibodies generated by *BT1927*-ON monoassociated mice only recognized *BT1927*-ON and not *BT1927*-OFF and vice versa. From our data, we found that the sera generated from *BT1927*-ON monoassociated mice recognized *BT1927*-ON and *BT1927*-OFF bacteria at a similar affinities as well as vice versa (**Figure 3.8**). We believe that these antibodies generated from monoassociated mice, although not strain-specific, are still specific to some part of *Bt,* since sera from GF mice controls show very little binding to both mutant strains (We think that some *BT1927*-ON or OFF specific antibody detected in the GF mice could be due to presence of natural antibodies). This suggests that the most immunogenic surface antigens are common to both mutants, although the surface architecture of the two mutants by TEM looks completely different.

Next, we compared the level of antibodies generated by each monoassociated mice, and found that both *BT1927*-ON and *BT1927*-OFF monoassociated mice generate a similar level of IgA, IgG1 and IgG3 that bind to both mutants. The exception is sera taken from Day 7 *BT1927*-ON monoassociated mice, which showed a higher level of IgG3 bound to both mutants than Day 7 sera from *BT1927*-OFF monoassociated mice (**Figure 3.8**). This could suggest that the *BT1927*-ON mutants are able to induce a quicker boost of IgG3 than *BT1927*-OFF mutants when they first colonize the mouse, which could be related to the observation that *BT1927*-ON are resistant to complement mediated lysis. The resistance to complement-mediated lysis could potentially allow *BT1927*-ON to colonize niches that are usually unavailable to *Bt,* leading to initiation of a more robust adaptive immune response.

No significant differences observed in the niche occupied by *BT1927*-ON and *BT1927*-OFF

We next performed fluorescent *in situ* hybridization (FISH) on the colon sections of *BT1927*-ON and *BT1927*-OFF monoassociated mice to determine whether there are differences in the niches that the mutants colonize in the mouse gut. Huang and coworkers have shown that a small percentage of a related bacterium *Bacteroides fragilis* colonizes the inner mucosal layer (relatively sterile, unavailable to other organisms such as *Escherichia coli*) by binding to mucin (89). They further hypothesized in their discussion that since only a small portion of the population are found in the inner mucus layer that the mucin binding properties may be controlled by a phase variation. We obtained colon tissue sections of *BT1927*-ON or *BT1927*-OFF monoassociated mice and subjected them to fluorescence *in situ* hybridization using a universal 16S rDNA probe published by others (90), counterstained the epithelial tissue with DAPI and observed the section under a fluorescent microscope. We were especially interested in whether the one mutant preferably colonized the lumen of the gut or more closely to the epithelial lining, as hypothesized by Huang et al. As reported by others (91), usage of Carnoy's fixative allowed us to observe the epithelial lining of the colon, the inner mucus layer, which appeared sterile, and the gut lumen where the majority of the bacteria were present. We occasionally found the sterile mucus layer being compromised by bacteria, especially more frequently in the colon tissue removed from the *BT1927*-ON monoassociated mice. However, this observation was never measured systematically so no statistics could be performed to show a statistical significance. Discussion with other groups who have performed FISH on GF mouse colon informed us that compared to conventional mice, GF mice often do show a breach in the inner mucus layer more frequently than the conventional mice with a normal microbiota, probably due to an underdevelopment of the immune system leading to insufficient amount of antimicrobial peptides or antibodies that keep the inner mucus layer intact (personal communication with Justin Sonnenburg and Kristen Ann Earle). In retrospect, we believe that the approach that we took (monoassociation) was perhaps not the best method to use in order to study a niche difference between the two mutants, since in monoassociation study, all of the niches are available for colonization by one strain of bacteria. The fact that there is no need to compete for niches might be masking the true condition for a niche tropism, if any, of the mutant strains. If we were to perform this study again, it is probably better to mix the two strains to let them compete, so the conditions will more closely mimic the conditions of a natural setting.

Materials and Methods

Human complement killing assay

Bt and mutant strains were cultured overnight in TYG medium. The next day, cells were harvested by centrifugation, washed once with PBS, and resuspended to 50 x 10^6 cfu/ml in PBS^{++} (PBS supplemented with 0.5 mM $MgCl_2$ and 1 mM $CaCl_2$). Cells were incubated in human serum and heat inactivated serum at various concentrations in PBS^{++} at 37 °C for 1 h. Following incubation, cells were diluted and plated on BHI + 10% horse blood agar plates and incubated anaerobically until colonies appeared. Percent survival was calculated by the dividing the average number of colonies that appeared on each

human serum plate by the average number of colonies that appeared on the heat-inactivated serum plate, multiplied by 100. Error bars represent the standard deviation. Student's t-Test was performed to calculate p-value. *P<0.05

Flow cytometry to determine C3 fragment presence in *BT1927*-ON and *BT1927*-OFF cells

BT1927-ON and *BT1927*-OFF were cultured overnight in TYG medium. Cells were pelleted, washed once with PBS, and approximately the same number of cells was incubated in 20% human serum in PBS^{++} for 30-60 min at 37°C. Following incubation, cells were pelleted and washed 3x with BSB. The cells were then stained with FITC-conjugated anti-human C3 $F(ab')_2$ (Protos Immunoresearch Cat. 365) at 1:50 final concentration, washed 3x with BSB and stained with 1:1000 SYTO 59 (Molecular Probes) for 1 h at 37 °C. Each sample was analyzed using the LSRII, gating on the top population that appeared on the FSC/SSC as described earlier. Spectral overlap was calculated from single-stained controls and a single-cell gate, and an APC+ gate were further set using unstained controls. The absolute number of events that were APC+FITC- (intact cells that lacked C3 fragments) was plotted on the bar graph for each serum concentration. Student's t-Test was performed to calculate the p-value. The histogram was generated by plotting the fluorescence intensity of FITC vs % max. Spectral overlap was calculated from single-stained controls. All post-acquisition analyses and compensations were performed using FlowJo (Tree Star).

Western blot to determine complement pathway

B. thetaiotaomicron strains were grown in TYG media overnight. The following day, the cells were washed once with PBS^{++}, and incubated in PBS^{++}, 20% human serum (Quidel #A112) in PBS^{++}, 20% human serum in PBS^{++} with or without 10mmM EDTA, or 10mM Mg-EGTA for 30 minutes at 37°C. After the incubation, the cells were placed on ice, and pelleted at max speed in the microcentrifuge. Then cells were washed five times with high salt PBS (PBS with 500mM) with protease inhibitors (Roche cOmplete mini EDTA-free protease inhibitor cocktail), resuspended in 2% SDS and incubated at 55°C for 20 minutes. BCA assays was performed to ensure equal loading and lysates were run on a 7.5% SDS-PAGE. The samples were transferred onto a nitrocellulose membrane and immunostained with goat anti-human C3-HRP (Cappel Research Products #ICN55237).

Bone marrow derived macrophage stimulation assay

10^6 bone marrow derived macrophages (BMM) were plated onto non-TC 12 well plates in RPMI complete media with no antibiotics (Recipe: 5 ml of 200 mM L-Glutamine, 5 ml of 100 mM Sodium pyruvate, 5 mL of 1M HEPES, 1.7 µL of β-mercaptethanol, and 50 ml of Fecal Calf Serum) and incubated overnight in the 37°C CO_2 incubator. *B. thetaiotaomicron* strains were grown in 5 ml of TYG media overnight in the anaerobic chamber at 37°C. The following day, bacteria were washed twice with PBS, and resuspended to 10^6 cells per ml of RPMI with no antibiotics. RPMI media was aspirated from the plates with macrophages, and 1 ml of each strain of bacteria, control ligands LPS

(TLR4 positive control), PAM3CSK (TLR2 positive control) or RPMI (for no stimulation control) were added. Plates were spun down for 2 min at 1200 rpm and incubated for 30 minutes in the 37°C CO_2 incubator. After the short incubation, Golgi plug (1.2 µL of Golgi plug resuspended in 200 µL of RPMI media) were added to each well and incubated for 4-5 hours in the 37°C CO_2 incubator. After the long incubation, the cells were transferred to FACS tubes, and stained with 75 µL of 780 Live/Dead stain (dissolved in PBS) at 4°C in the dark for 15 minutes. Macrophages were washed once with FACS buffer (500 ml PBS, 5 ml of FBS, 2.5 ml of 20% Sodium Azide and 1 ml of 0.5M EDTA) and fixed with BD Perm (BD Cytofix/Cytoperm TM Fixation and Permeabilization Solution Sold as 554722 Cat # 51-2090KZ, Lot# 2312862) for 20 minutes in the dark at 4°C. After the incubation, cells were washed with FACS buffer twice. Fc receptor was blocked by incubating the cells in 50µL of 1:250 2x Fc-block in FACS buffer for 10 minutes on ice. 50 µL of 1:200 anti-mouse TNFα-PE (Clone:MP6-XT22, Cat# 12-7321-82, Lot# E02144-1630 0.2mg/ml from eBioscience) in BD Perm Wash (51-2091KZ, Lot: 2243921 from BD) were added and incubated on ice for 20 minutes. Finally, cells were washed with BD Perm wash twice and analyzed on the BD LSR Fortessa.

Real-time measurement of *B. thetaiotaomicron* strain growth in LL-37

The experimental procedure used were published by Eini et al. (92). *B. thetaiotaomicron* strains were grown in 5 ml of TYG media overnight in the anaerobic chamber at 37°C. OD of the overnight cultures was measured to ensure similar level of confluency. The confluent cultures was diluted 1:200 with freshly made TYG containing 0 (PBS only), 0.5, 1.0, 5, 10, 20, or 40 µg/ml of LL-37 dissolved in PBS. 200 ul of this diluted culture with LL-37 were added to each well in a 96 well plate, keeping columns 1 and 12 empty. Then, the following procedures were performed in the anaerobic chamber. In order to make this plate anaerobic, 8 wells in column 1 and 8 well in column 12 were filled with the anaerobic generating substance from an AnaeroGen™ Atmosphere Generation System (Oxoid, UK). The plate was sealed by putting the cover on with petroleum jelly (Vaseline) injected from a 50 mL syringe in between the lid and the plate to ensure gas-tightness. Oxygen elimination was monitored by resazurin included in the TYG media (resazurin turn clear when the environment in anaerobic, pink in aerobic conditions). The plate was inserted into the TECAN set in an aerobic environment, and real time measurement of bacterial growth in various concentrations of LL-37 was measured every 30 minutes at 37°C for approximately 24 hours.

Monoassociation of GF mice

All mouse experiments were performed under the approval of the institutional review board at Stanford University. *BT1927*-ON and *BT1927*-OFF were grown in TYG overnight in the anaerobic chamber at 37°C. The following day, six Swiss-Webster germ free mice less than 12 weeks old were gavaged with *BT1927*-ON or *BT1927*-OFF cultures. Feces and serum were collected on Day 7 and Day 14 post-inoculation. On Day 14, two mice were sacrificed and their cecal contents, as well as their ileum, cecum and colon were collected.

Fecal genomic DNA extraction and qPCR for verifying *B. thetaiotaomicron* colonization

Genomic DNA was extracted from fecal pellets collected using the ZR Fecal DNA Miniprep kit from Zymo, according to the manufacture's instructions. 100 ng of each fecal genomic DNA was added into a 20 µL qPCR reaction with Sybr Green Master Mix and *B. thetaiotaomicron* specific 16S primers (**Table 3.1**). Reactions were run on the Light Cycler 480 real time PCR machine.

Bacterial flow cytometry to measure level of specific antibodies generated against *BT1927*-ON and *BT1927*-OFF

One pellet of fresh feces were homogenized and vortexed in 500 µl of sterile PBS and filtered (0.45 µm) into one well of a 12 well plate. Bacteria were rinsed through the filter with PBS for a total of two washes. The bacteria were transferred to an eppendorf tube, washed again with PBS and then resuspended to approximately $50x10^6$ cfu/mL in BSB. 25 µl of serum diluted 1:25 in BSB were mixed with 25 µl of $50x10^6$ cfu/ml of bacteria in v-bottom 96-well plates and incubated for 1 hour at 4°C. After the incubation, cells were washed by addition of 150 ul of BSB followed by centrifugation at 4000 rpm for 4 minutes at 4°C. Total of two washes were performed. After the two washes, 50 µL of 0.22 µm filtered anti-mouse Ig antibodies (BD Pharmingen anti-IgG1-APC Clone A85-1 Cat#560089, BD Pharmingen Biotin Rat anti-mouse IgG3 Clone R40-82 Cat# 553401, Southern Biotech Rat anti-mouse IgA-RPE Clone 11-44-2 Cat#1165-09) were added and incubated for 30 minutes at 4°C. Following the short incubation, stained cells were washed with BSB twice, again with 150 µL of BSB, followed by centrifugation at 4000 rpm for 4 min at 4°C for a total of two times. 0.22 µm filtered secondary antibody SA-PECy7 diluted 1:200 in BSB were added and incubated for 20 minutes at 4°C. After the incubation, stained cells were washed twice with BSB as before. Finally, cells were resuspended in 0.22 µm filtered PBS supplemented with 2% paraformaldehyde and analyzed on the BD LSR Fortessa. Compensations were performed using the BD CompBeads Compensation Particles Anti-Rat/Hamster Ig,κ/Negative Control (BSA*) Set (Cat# 552845).

Tissue fixation, paraffin embedding and sectioning

Colon tissue preservation and were performed according to Johansson and Hansson (90) in order to preserve the mucus layer of the intestine. Briefly, mice were sacrificed, and the intestine was dissected and placed into a tube with methanol-Carnoy's fixative. The tissue was fixed in this solution for 3 hours and kept in solution for up to 2 weeks at room temperature. The fixed tissue was washed in dry-methanol, 30 minutes each for two times, followed by absolute ethanol wash for 20 minutes each for two times. Finally, tissues were incubated in two baths of xylene for 15 minutes, embedded in paraffin and sectioned in 4 µm thin sections and placed on glass microscope slides.

Fluorescent *in situ* hybridization (FISH)

FISH were performed according to Johansson and Hansson (90). Briefly, sections on glass slides were dewaxed by incubating in 60°C oven for 10 minutes, followed by two 10 minute incubations in xylene substitute solution (Citrisolv) prewarmed to 60 °C. Sections were incubated in 99.5% Ethanol for 5 minutes, and the slides were dried. 50 µL of hybridization solution (20mM Tris-HCl, pH7.4, 0.9M NaCl, 0.1%(w/v) SDS) with 0.5 µg of EUB probe conjugated to TYE-665 on the 5'(IDT; 5' /TYE665/GCTGCCTCCCGTAGGAGT-3') prewarmed to 50 °C were dropped onto the slide. A coverslip was placed on top of the slide, and the slide was placed in a humidified chamber and incubated overnight in 50°C. The next morning, the cover glass was removed and the slides were washed in FISH washing buffer at 50°C for 10-20 minutes, followed by three PBS washes. Slides were almost completely dried and mounted using an antifade mounting media. A coverslip was placed and sealed using clear nail polish and the slide were viewed under a fluorescent microscope using appropriate filters.

Figures and Tables

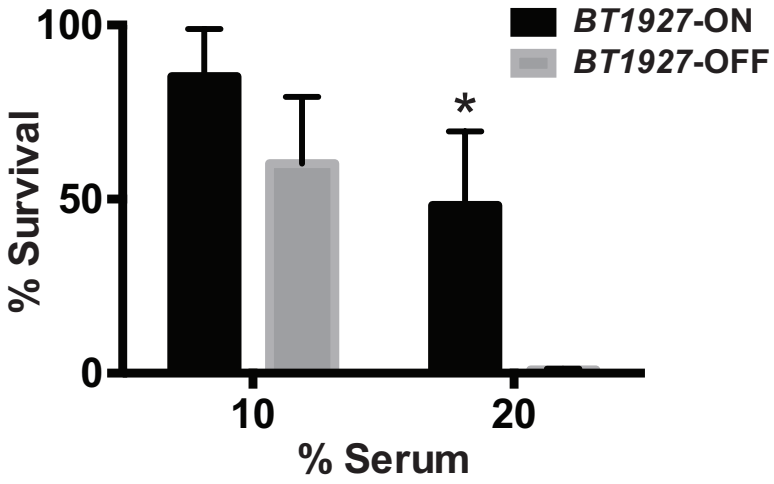

Figure 3.1 BT1927 confers resistance to complement-mediated killing. *BT1927*-ON and *BT1927*-OFF cells were incubated in 10% or 20% human serum at 37 °C for 1 h, serially diluted and plated. The number of colonies that appeared on the plates was counted to calculate percent survival. In 20% serum, *BT1927*-ON were more resistant to serum-mediated-lysis (48.18 ± 12% survival) than *BT1927*-OFF cells (0.97 ± 0.18% survival). Error bars show standard deviation (n = 3). *P<0.05 Student's t-Test.

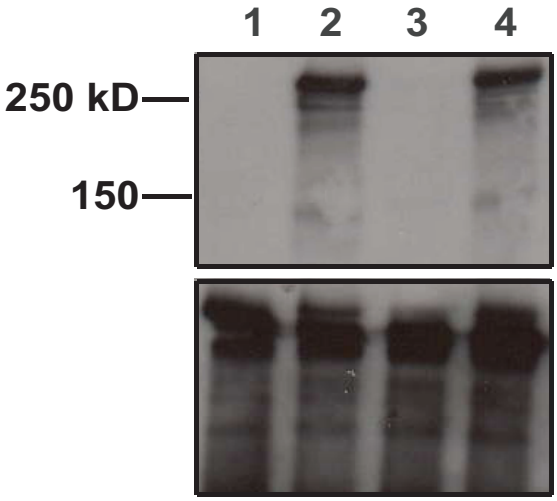

Figure 3.2 *Bt* activates the alternative pathway. Western blot of *Bt* stained with anti-C3 antibody where (1) cells with only buffer, (2) cells with 20% human serum, (3) cells with human serum and 10mM EDTA, and (4) cells with human serum and 10mM Mg-EGTA. Bottom panels shows the samples but stained with anti-*B. thetaiotaomicron* antiserum as a loading control.

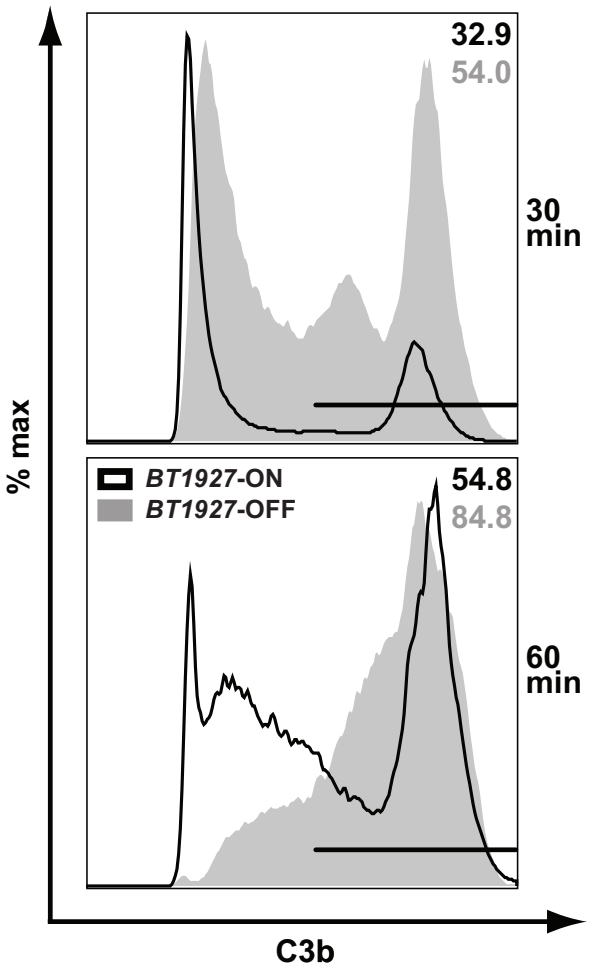

Figure 3.3 *BT1927*-ON cells appear to activate the complement with delayed kinetics. The same experiment as described in Figure 3.3 was used to measure the distribution of FITC+ (C3 fragment-associated) and FITC- (not C3 fragment-associated) populations in the *BT1927*-ON and *BT1927*-OFF mutants. Samples were treated with 10% serum for 30 min (top panel) or 60 min (bottom panel). The results show that *BT1927*-ON cells appear to activate complement with delayed kinetics compared with the *BT1927*-OFF cells, as measured by presence of C3 fragment.

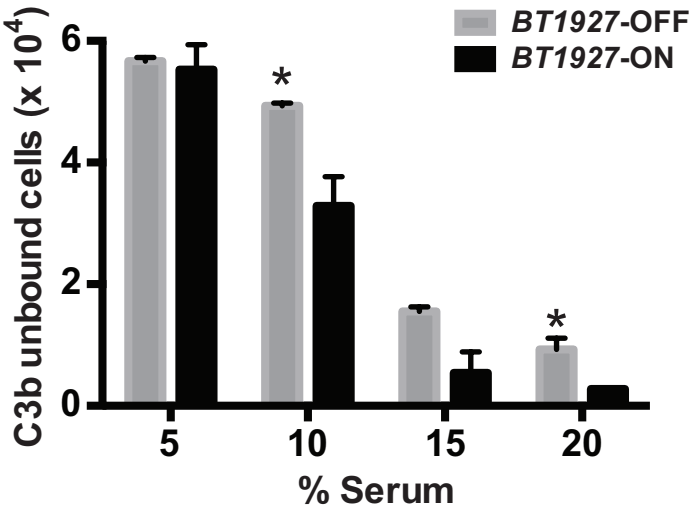

Figure 3.4 *BT1927*-ON cells bind less to C3b. Approximately the same number of *BT1927*-ON and *BT1927*-OFF cells were incubated in 5%, 10%, 15%, or 20% serum at 37 °C for 30 min, washed, stained with FITC-conjugated anti-C3 $F(ab')_2$ and analyzed by flow cytometry. The bar graph shows the absolute number of events that were APC+FITC- (intact cells not associated with C3 or a C3 fragment). C3 or its fragments associate with *BT1927*-ON cells at lower efficiency relative to *BT1927*-OFF cells, consistent with a blockade of C3b deposition by BT1927. Error bars show standard deviation (n = 2). *P<0.05 Student's t-Test.

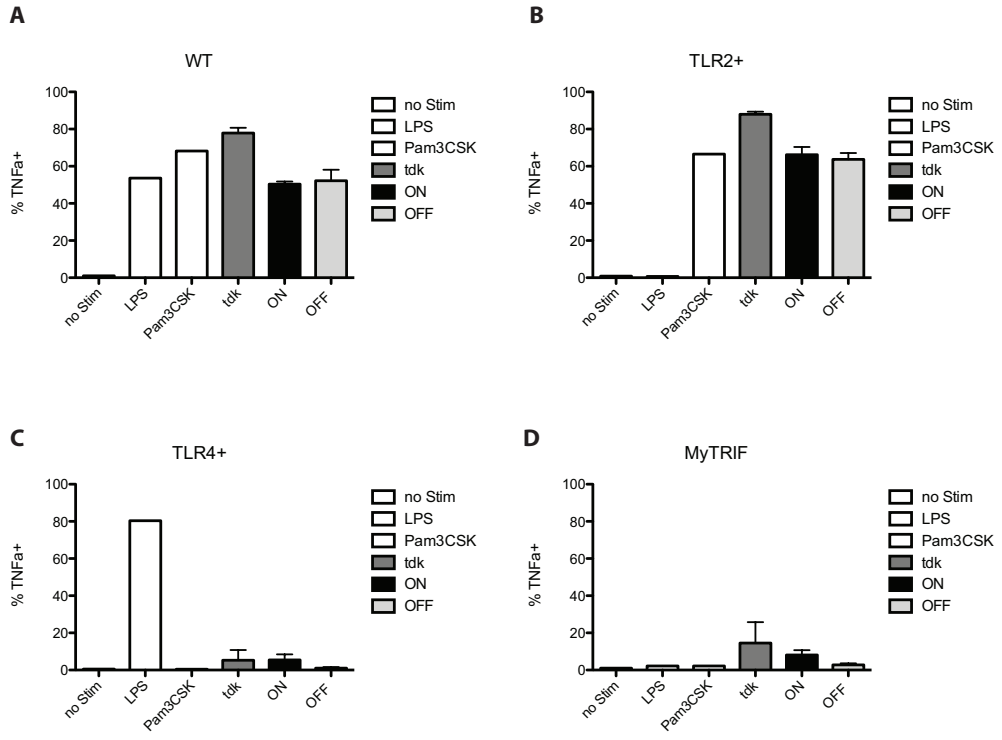

Figure 3.5 TLR activation assay using bone marrow derived macrophages. Panels show the average percentage of bone marrow derived macrophages with positive intracellular TNFα staining after incubation with *BT1927*-ON, *BT1927*-OFF or controls. The four panels shows various macrophages which were differentiated from bone marrows derived from (A) wildtype, (B) TLR2 only, (C) TLR4 only, or (D) TRIF/MyD88 KO mice. From this result, *Bt*, *BT1927*-ON and *BT1927*-OFF appear to activate TNFα mostly through the TLR2 pathway, and there are no differences in the level of activation among the strains. Error bar represents SEM of three technical replicates.

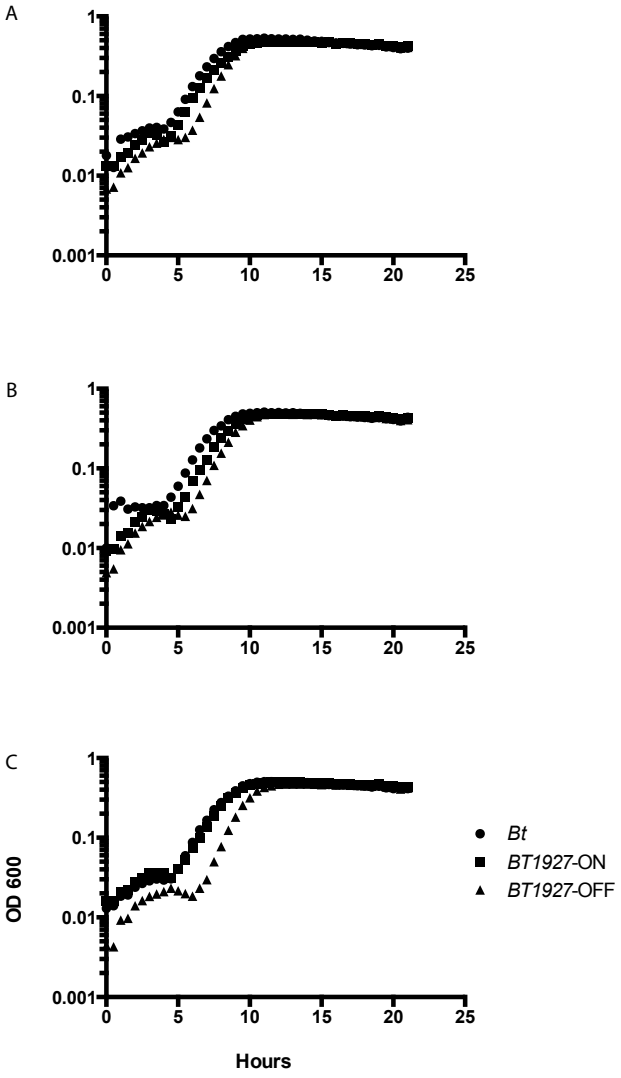

Figure 3.6 Growth curve of *B. thetaiotaomicron* strains in the presence of antimicrobial peptide LL-37. Panel shows growth curve of *Bt, BT1927*-ON and *BT1927*-OFF in TYG media with (A) PBS; (B) 0.5 μg/ml of LL-37; and (C) 1 μg/ml of LL-37. Notice there is slight increase in lag phase in *BT1927*-OFF at 1 μg/ml of LL-37 but not *BT1927*-ON. Each point represents the average absorbance of three replicates taken at the indicated time. Error bars represent standard deviation (SD).

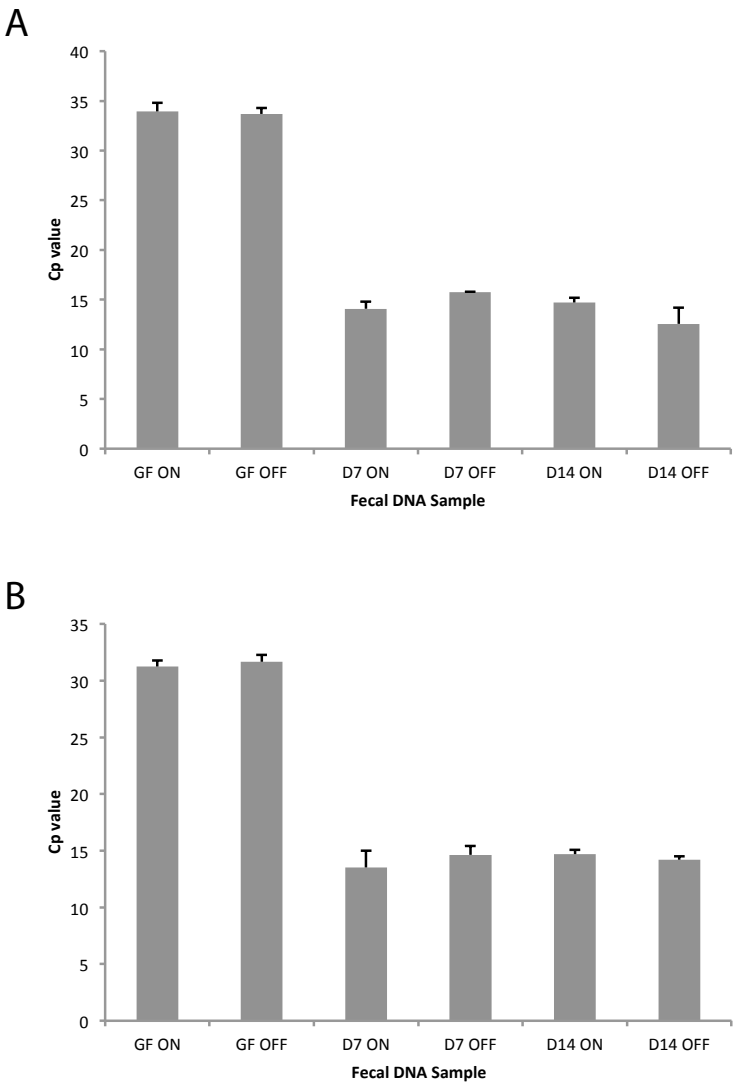

Figure 3.7 Enumeration of *BT1927*-ON and *BT1927*-OFF colonization levels in monoassociated mice. Both panels show average Cp values from quantitative PCR results performed on genomic DNA extracted from respective GF mice or monoassociated mice using *Bt* specific 16S primers set 1 (A) or set 2 (B). Error bars show standard error of mean (SEM) of three biological replicates (three different mouse feces per condition).

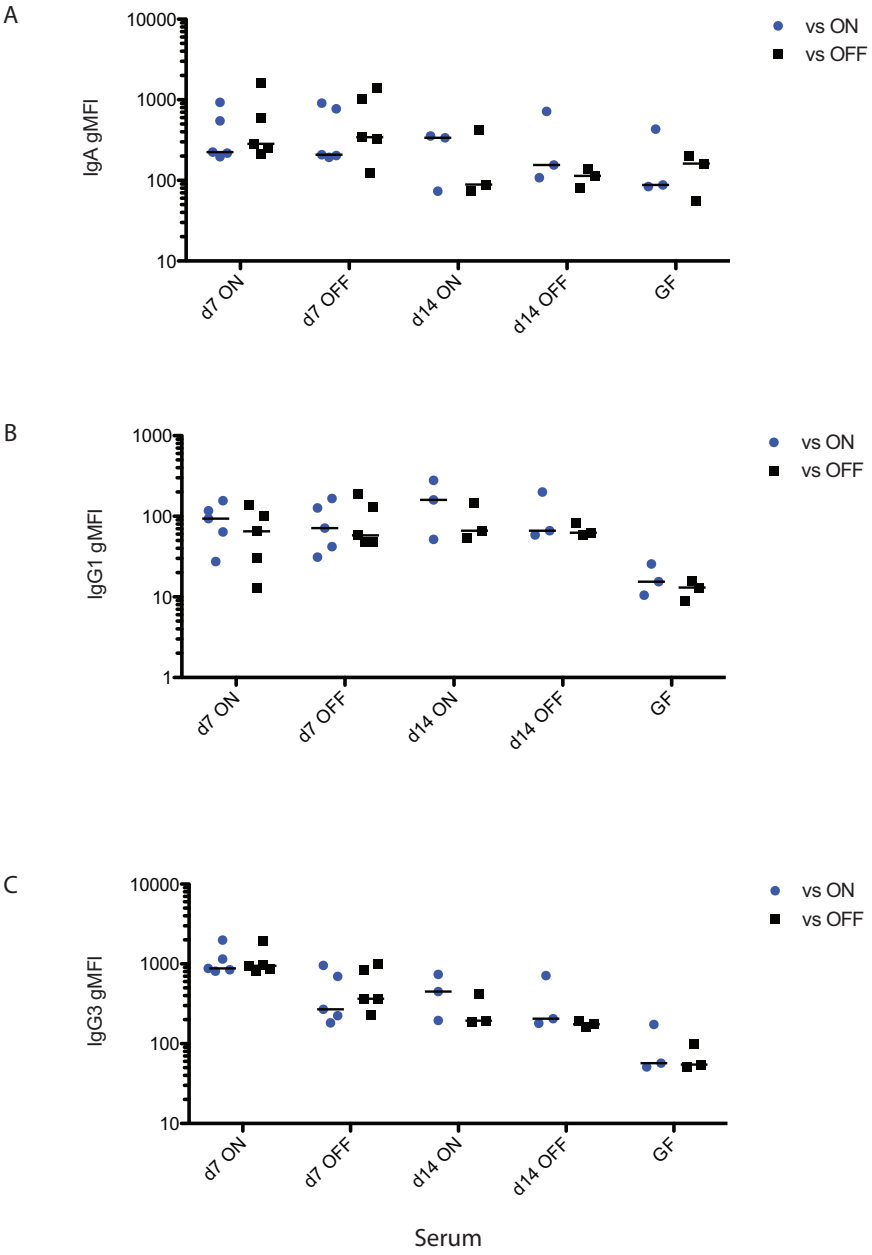

Figure 3.8 *BT1927*-ON and *BT1927*-OFF specific IgA, IgG1, and IgG3 levels in monoassociated mice. *BT1927*-ON or *BT1927*-OFF bacteria were isolated from feces from monoassociated mice or GF mice and were labeled with the respective mouse serum. The labeled bacteria were further stained to measure the level of antibody response via flow cytometry. Panel (A) shows response for IgA, (B) for IgG1 and (C) for IgG3. Each point represents one fecal pellet from a monoassociated mouse. gMFI = geometric mean fluorescence intensity.

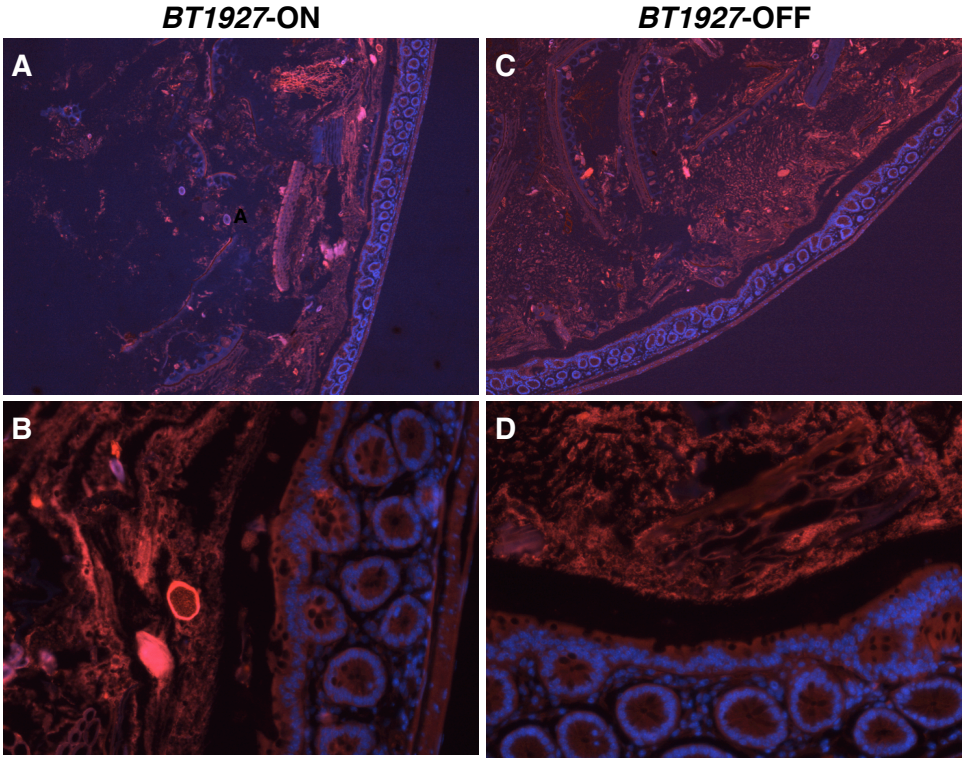

Figure 3.9 FISH labeled colon tissue section of *BT1927*-ON and *BT1927*-OFF monoassociated mice. Colon tissue sections from (A) and (B) *BT1927*-ON and (B) and (C) *BT1927*-OFF monoassociated mice were subject to fluorescent *in situ* hybridization using a 16s universal rDNA probe conjugated to TYE-665 (red) to detect bacteria in the colon. The sections were counterstained with DAPI (blue). (A) and (C) are images taken at 40X magnification and (B) and (D) are images taken at 100X magnification. The almost 'sterile' mucus layer was observed throughout the colon, although some areas were compromised with invading bacteria.

Primer	Sequence
16S-F4	GTGTAGCGGTGAAATGCTTAGATATC
16S-R4	CAGTGTCAGTTGCAGTCCAGTGA
16S-F7	GGTAGTCCACACAGTAAACGATGAA
16S-R7	CCCGTCAATTCCTTTGAGTTTC

Table 3.1 List of *B. thetaiotaomicron* specific 16s primers used in this study.

Chapter 4 : Conclusion and Future Directions

Conclusion

Bacteroides capsules have been a model system for studying the molecular mechanisms of host-commensal interactions for the last decade. These extracellular polysaccharide capsules are encoded by a set of phase-variable biosynthetic gene clusters in which one of them–polysaccharide A–has been well studied and shown to have anti-inflammatory properties. This *symbiosis factor* is thought to play an important role for the organism's survival and maintenance inside the human host. This dissertation reports on the serendipitous discovery of a new protein based capsule that is strikingly different in appearance from known polysaccharide capsules and discusses the mechanism of expression and the potential role it could play during colonization and growth inside the mammalian host.

Chapter 2 of the dissertation describes our experience of observing the phenomenon of phase variation. In the process of characterizing a locus that was predicted to encode a surface structure, we serendipitously discovered a phase-variable protein of unknown function–BT1927–that is expressed in a subpopulation of ~1:1000 cells in laboratory culture of *B. thetaiotaomicron.* Transmission electron micrographs of cells expressing BT1927 show a hexagonally tessellated surface layer that is striking in appearance and unprecedented in *Bacteroides.* The discovery of this novel proteinaceous capsule in *B. thetaiotaomicron* demonstrates that *Bacteroides* is capable of completely remodeling its surface to replace the more common polysaccharides, and reveals that the *Bacteroides* capsule is more versatile and varied in composition than had previously been recognized. This is an unanticipated finding that reminds us of how many basic, fundamental elements remain to be discovered in *Bacteroides*, the genus that comprises >50% of the cells in a typical human gut community.

In chapter 3, the possible function of the *BT1927*-expressing subpopulation during colonization and growth of the organism in the mammalian host is explored. *B. thetaiotaomicron* mutants in which the expression of *BT1927* had been 'locked' on and off by mutating one of the inverted repeats flanking its promoter were subjected to relevant *in vitro* and *in vivo* assays to find a differential phenotype. Of all the assays we tried (recognition by IgA, tropism in the small and large intestine, sensitivity to antimicrobial peptides, activation of TLR2 and TLR4, and sensitivity to lysis in serum), one significant difference was reproduced: *BT1927*-ON cells are profoundly more resistant to complement-mediated killing compared to *BT1927*-OFF cells. This finding is especially intriguing in light of recent evidence of a role for complement in modulating the composition of the skin, oral and gut communities.

The results of the two chapters raise the question of what advantage does *B. thetaiotaomicron* have by regulating *BT1927* in a phase-variable manner. If BT1927 confers resistance to complement, which is clearly an advantage to the bacteria, why would the bacteria switch it on and off or have it present only in a minority of the population? We hypothesize that *BT1927* is only present in the minority of the population because the bacteria has evolved to maintain a diverse set of surface structures (including *BT1927*, but also other surface structures like the polysaccharide capsules) in order to maximize the probability of surviving various catastrophic events such as complement, opsonization,

phage attack, etc. Although expressing the S-layer protein maybe advantageous in one setting, having them or the lacking other surface structures, such as the polysaccharide capsules, may be disadvantageous in another setting. Therefore, rather than committing an entire population to express S-layers, maintaining a heterogeneous population with diverse surface structures is better for the entire population. The reversible switch also allows the entire population to adapt to a particular situation without committing to it. For example, if a host has a major inflammatory response and suddenly complement is deposited in the gut, the S-layer ON population will survive with a greater probability. And once the complement cascade has ended, and the robust inflammatory response has dampened, the S-layer ON cells that survived can perhaps repopulate the entire population, and can turn off the S-layer promoter and turn on other surface structures that might be needed in other situations, increasing the surface diversity again.

In *Bacteroides fragilis* (and probably other *Bacteroides* species), simultaneous expression of the multiple polysaccharide capsules is inhibited by the transcription inhibitors UpxZs. Each of the eight UpxZs have a different inhibitory spectra and establishes a hierarchical regulatory network allowing a single strain of *B. fragilis* to produce cells expressing one of each of the eight distinct surface polysaccharide PSA through PSH (35). The potential significance of the maintenance of this diversity is illustrated by the study that Comstock and coworkers performed (48) in which the percentage of the orientation of each polysaccharide locus promoter was measured in broth, in monoassociated mice, in conventional mice and in mice with abscess. The percentage of PSH ON population was low in broth, but increased to ~100% when the bacteria was inoculated into germfree mice, suggesting its importance during colonization. The percentage in a different polysaccharide, PSA, the ON population was 50-80% in broth and in monoassociated mice. However, after the bacteria was introduced into conventional (complex flora) mice, one of the litters decreased to ~0% suggesting that PSA expression is not preferred in a complex flora. These results support the idea that a particular surface structure could be advantageous in one setting and disadvantageous in another setting.

Uropathogenic *Escherichia coli* (UPEC) also possess phase-variable fimbriae necessary for adherence in urinary tract infections (UTI). UPEC has a phase-variable type I fimbriae which its expression is controlled in a similar manner to *BT1927*. Mobley and coworkers (52) measured the percentage of orientation of the Uropathogenic *E.coli* in an UTI model and found that the type I fimbriae Locked-ON mutants are much more competitive during the first 24 hour of infection compared to the Locked-OFF mutants. However, as the bacteria ascend the ureter to the kidneys, another fimbriae called P-fimbriae become an important virulence factor for colonizing the kidneys. During this time, P-fimbriae actually downregulate the expression of type I fimbriae because to the polysaccharides in *B. fragilis,* a UPEC cell can only express one type of fimbriae at a time. Therefore, it is thought that the majority of the cells turn off the type I-fimbriae and turn on the P-fimbriae, supporting the idea that diverse surface structures are necessary for various settings and functions, and the reversibility allows the entire population to adapt to the exact situation without full commitment.

Future Directions

The discovery of a novel proteinaceous capsule in *Bacteroides thetaiotaomicron* presented by this dissertation gives rise to more questions about the basic biology of the capsules in *Bacteroides*.

First, in the transmission electron micrographs, the proteinaceous tessellated capsule appears as if it has replaced the more common electron dense polysaccharide capsule. The question then becomes, where are the polysaccharide capsules in the *BT1927*-expressing cells? Are polysaccharide capsules still present? If they are, where did they go? If they are not present, is there some regulatory mechanism that prevents expression of the polysaccharide capsule when the proteinaceous capsule is on? One way to address these questions might be to create an antibody against polysaccharide capsules, and perform a western blot of *BT1927* expressing whole lysates and determine whether the antibodies detect polysaccharides in the *BT1927* expressing cells. We attempted this exact experiment using anti-serum against wildtype *B. thetaiotaomicron* (not specific to polysaccharides) but it was inconclusive due to the fact that we could not find a difference between the *BT1927* expressing cells and *BT1927* off cells. In order to determine whether there is a mutually exclusive type of regulation, one could simultaneously use the antibody specifically against polysaccharides and an antibody specifically against BT1927 to see if the expression of BT1927 inhibits the expression of polysaccharides.

Second, the dissertation explored the mechanism of how the promoter flipping turns the S-layer protein expression on and off. Although we attempted to explore conditions in which the promoter flips, we were never able to find one. So the question of "when does the S-layer turn on?" still remains to be answered. One way to begin addressing this question is to look at when the site-specific recombinase that is most likely flipping the promoter turns on. There are some regulatory elements upstream of the site-specific recombinase, such as a sequence similar to that of the csgD box from *E. coli* (93) which could be clues to the trigger needed to turn on the site-specific recombinase and consequently turn on the S-layer protein expression.

Third, this dissertation explored only one of the 20 predicted phase-variable sites where most have an unknown function (94). What do the other phase-variable sites annotated as hypothetical surface proteins encode? One can begin to explore the phase-variable sites in other parts of the genome by attempting to 'lock' as many sites and performing transmission electron microscopy to determine whether any other novel surface structures are formed. When we performed transmission electron microscopy on *BT1927*-ON and *BT1927*-OFF as well as the wildtype strain, we did see a few other surface variants that looked different from the S-layer we found and the more common polysaccharide capsule. These surface variants could be present as a result of phase-variable genes in another part of the *B. thetaiotaomicron* genome. Furthermore, it would be interesting to expand this exploration into other *Bacteroides* species, such as *Bacteroides ovatus, and Bacteroides vulgatus*, which are most common among the human gut communities.

Fourth, the finding of BT1927, an extracellularly secreted protein, opens up a new project on studying secreted proteins in *Bacteroides*. The signal peptide and the abundance

of the cut protein in the media supernatant, along with the adjacent gene predicted to be an outer membrane protein with beta-barrel structure, suggests that BT1927 is secreted by a two-partner secretion system. Although the exact mechanism of secretion has not been explored in this dissertation. The study of how this S-layer protein is secreted will be very exciting, especially since it could potentially be applied as a therapeutic delivery system for delivering drugs into the lumen of the mammalian gut.

Finally, there are other potential functions of the S-layer that have not been addressed in this dissertation. Other functions that one could explore include: protection from bacteriophage, biofilm formation (S-layer expressing cells could be involved in formation of biofilms) and microbe-to-microbe interaction (S-layer expressing cells could be more resistant to small molecules such as antibiotics made by other bacteria during competition of niches).

References

1. **Macpherson AJ, Harris NL**. 2004. Interactions between commensal intestinal bacteria and the immune system. Nat Rev Immunol **4**:478–485.
2. **Hooper LV**. 2009. Do symbiotic bacteria subvert host immunity? Nat Rev Micro **7**:367–374.
3. **Blaser M, Bork P, Fraser C, Knight R, Wang J**. 2013. The microbiome explored: recent insights and future challenges. Nat. Rev. Microbiol. **11**:213–217.
4. **Donia MS, Cimermancic P, Schulze CJ, Wieland Brown LC, Martin J, Mitreva M, Clardy J, Linington RG, Fischbach MA**. 2014. A Systematic Analysis of Biosynthetic Gene Clusters in the Human Microbiome Reveals a Common Family of Antibiotics. Cell **158**:1402–1414.
5. **Turnbaugh PJ, Ley RE, Hamady M, Fraser-Liggett CM, Knight R, Gordon JI**. 2007. The Human Microbiome Project. Nature **449**:804–810.
6. **Turnbaugh PJ, Gordon JI**. 2009. The core gut microbiome, energy balance, and obesity. J. Physiol.
7. **Arumugam M, Raes J, Pelletier E, Le Paslier D, Yamada T, Mende DR, Fernandes GR, Tap J, Bruls T, Batto J-M, Bertalan M, Borruel N, Casellas F, Fernandez L, Gautier L, Hansen T, Hattori M, Hayashi T, Kleerebezem M, Kurokawa K, Leclerc M, Levenez F, Manichanh C, Nielsen HB, Nielsen T, Pons N, Poulain J, Qin J, Sicheritz-Ponten T, Tims S, Torrents D, Ugarte E, Zoetendal EG, Wang J, Guarner F, Pedersen O, de Vos WM, Brunak S, Doré J, MetaHIT Consortium (additional Members), Weissenbach J, Ehrlich SD, Bork P**. 2011. Enterotypes of the human gut microbiome. Nature **473**:174–180.
8. **Consortium THMP**. 2012. A framework for human microbiome research. Nature **486**:215–221.
9. **Consortium THMP**. 2012. Structure, function and diversity of the healthy human microbiome. Nature **486**:207–214.
10. **Honda K, Littman DR**. 2012. The Microbiome in Infectious Disease and Inflammation. Annu. Rev. Immunol. **30**:759–795.
11. **Qin J, Li Y, Cai Z, Li S, Zhu J, Zhang F, Liang S, Zhang W, Guan Y, Shen D, Peng Y, Zhang D, Jie Z, Wu W, Qin Y, Xue W, Li J, Han L, Lu D, Wu P, Dai Y, Sun X, Li Z, Tang A, Zhong S, Li X, Chen W, Xu R, Wang M, Feng Q, Gong M, Yu J, Zhang Y, Zhang M, Hansen T, Sanchez G, Raes J, Falony G, Okuda S, Almeida M, LeChatelier E, Renault P, Pons N, Batto J-M, Zhang Z, Chen H, Yang R, Zheng W, Li S, Yang H, Wang J, Ehrlich SD, Nielsen R, Pedersen O, Kristiansen K, Wang J**. 2012. A metagenome-wide association study of gut microbiota in type 2 diabetes. Nature **490**:55–60.
12. **Mulle JG, Sharp WG, Cubells JF**. 2013. The Gut Microbiome: A New Frontier in Autism Research. Curr. Psychiatry Rep. **15**:337.
13. **Gevers D, Kugathasan S, Denson LA, Vázquez-Baeza Y, Van Treuren W, Ren B, Schwager E, Knights D, Song SJ, Yassour M, Morgan XC, Kostic AD, Luo C, González A, McDonald D, Haberman Y, Walters T, Baker S, Rosh J, Stephens M, Heyman M, Markowitz J, Baldassano R, Griffiths A, Sylvester F, Mack D, Kim S, Crandall W,**

Hyams J, Huttenhower C, Knight R, Xavier RJ. 2014. The Treatment-Naive Microbiome in New-Onset Crohn's Disease. Cell Host Microbe **15**:382–392.
14. **Ley RE, Bäckhed F, Turnbaugh P, Lozupone CA, Knight RD, Gordon JI**. 2005. Obesity alters gut microbial ecology. Proc. Natl. Acad. Sci. U. S. A. **102**:11070–11075.
15. **Turnbaugh PJ, Ley RE, Mahowald MA, Magrini V, Mardis ER, Gordon JI**. 2006. An obesity-associated gut microbiome with increased capacity for energy harvest. Nature **444**:1027–131.
16. **Wang Z, Klipfell E, Bennett BJ, Koeth R, Levison BS, DuGar B, Feldstein AE, Britt EB, Fu X, Chung Y-M, Wu Y, Schauer P, Smith JD, Allayee H, Tang WHW, DiDonato JA, Lusis AJ, Hazen SL**. 2011. Gut flora metabolism of phosphatidylcholine promotes cardiovascular disease. Nature **472**:57–63.
17. **Koeth RA, Wang Z, Levison BS, Buffa JA, Org E, Sheehy BT, Britt EB, Fu X, Wu Y, Li L, Smith JD, DiDonato JA, Chen J, Li H, Wu GD, Lewis JD, Warrier M, Brown JM, Krauss RM, Tang WHW, Bushman FD, Lusis AJ, Hazen SL**. 2013. Intestinal microbiota metabolism of l-carnitine, a nutrient in red meat, promotes atherosclerosis. Nat. Med. **19**:576–585.
18. **Van Nood E, Vrieze A, Nieuwdorp M, Fuentes S, Zoetendal EG, de Vos WM, Visser CE, Kuijper EJ, Bartelsman JFWM, Tijssen JGP, Speelman P, Dijkgraaf MGW, Keller JJ**. 2013. Duodenal Infusion of Donor Feces for Recurrent Clostridium difficile. N. Engl. J. Med. **368**:407–415.
19. **Kelly CP**. 2013. Fecal Microbiota Transplantation — An Old Therapy Comes of Age. N. Engl. J. Med. **368**:474–475.
20. **Hooper LV, Littman DR, Macpherson AJ**. 2012. Interactions Between the Microbiota and the Immune System. Science **336**:1268–1273.
21. **Smith K, McCoy KD, Macpherson AJ**. 2007. Use of axenic animals in studying the adaptation of mammals to their commensal intestinal microbiota. Semin. Immunol. **19**:59–69.
22. **Ivanov II, Atarashi K, Manel N, Brodie EL, Shima T, Karaoz U, Wei D, Goldfarb KC, Santee CA, Lynch SV, Tanoue T, Imaoka A, Itoh K, Takeda K, Umesaki Y, Honda K, Littman DR**. 2009. Induction of Intestinal Th17 Cells by Segmented Filamentous Bacteria. Cell **139**:485–498.
23. **Gaboriau-Routhiau V, Rakotobe S, Lécuyer E, Mulder I, Lan A, Bridonneau C, Rochet V, Pisi A, Paepe MD, Brandi G, Eberl G, Snel J, Kelly D, Cerf-Bensussan N**. 2009. The Key Role of Segmented Filamentous Bacteria in the Coordinated Maturation of Gut Helper T Cell Responses. Immunity **31**:677–689.
24. **Garland CD, Lee A, Dickson MR**. 1982. Segmented filamentous bacteria in the rodent small intestine: Their colonization of growing animals and possible role in host resistance toSalmonella. Microb. Ecol. **8**:181–190.
25. **Heczko U, Abe A, Finlay BB**. 2000. Segmented Filamentous Bacteria Prevent Colonization of Enteropathogenic Escherichia coli O103 in Rabbits. J. Infect. Dis. **181**:1027–1033.
26. **Atarashi K, Tanoue T, Shima T, Imaoka A, Kuwahara T, Momose Y, Cheng G, Yamasaki S, Saito T, Ohba Y, Taniguchi T, Takeda K, Hori S, Ivanov II, Umesaki Y, Itoh K, Honda K**. 2010. Induction of Colonic Regulatory T Cells by Indigenous Clostridium Species. Science 1198469.

27. **Atarashi K, Tanoue T, Oshima K, Suda W, Nagano Y, Nishikawa H, Fukuda S, Saito T, Narushima S, Hase K, Kim S, Fritz JV, Wilmes P, Ueha S, Matsushima K, Ohno H, Olle B, Sakaguchi S, Taniguchi T, Morita H, Hattori M, Honda K**. 2013. Treg induction by a rationally selected mixture of Clostridia strains from the human microbiota. Nature **500**:232–236.
28. **Mazmanian SK, Round JL, Kasper DL**. 2008. A microbial symbiosis factor prevents intestinal inflammatory disease. Nature **453**:620–625.
29. **Mazmanian SK, Kasper DL**. 2006. The love-hate relationship between bacterial polysaccharides and the host immune system. Nat Rev Immunol **6**:849–858.
30. **Mahowald MA, Rey FE, Seedorf H, Turnbaugh PJ, Fulton RS, Wollam A, Shah N, Wang C, Magrini V, Wilson RK, Cantarel BL, Coutinho PM, Henrissat B, Crock LW, Russell A, Verberkmoes NC, Hettich RL, Gordon JI**. 2009. Characterizing a model human gut microbiota composed of members of its two dominant bacterial phyla. Proc. Natl. Acad. Sci. U. S. A. **106**:5859–5864.
31. **Krinos CM, Coyne MJ, Weinacht KG, Tzianabos AO, Kasper DL, Comstock LE**. 2001. Extensive surface diversity of a commensal microorganism by multiple DNA inversions. Nature **414**:555–558.
32. **Coyne MJ, Weinacht KG, Krinos CM, Comstock LE**. 2003. Mpi recombinase globally modulates the surface architecture of a human commensal bacterium. Proc. Natl. Acad. Sci. **100**:10446–10451.
33. **Weinacht KG, Roche H, Krinos CM, Coyne MJ, Parkhill J, Comstock LE**. 2004. Tyrosine site-specific recombinases mediate DNA inversions affecting the expression of outer surface proteins of Bacteroides fragilis. Mol. Microbiol. **53**:1319–1330.
34. **Chatzidaki-Livanis M, Coyne MJ, Comstock LE**. 2009. A Family of Transcriptional Antitermination Factors Necessary for Synthesis of the Capsular Polysaccharides of Bacteroides fragilis. J. Bacteriol. **191**:7288–7295.
35. **Chatzidaki-Livanis M, Weinacht KG, Comstock LE**. 2010. Trans locus inhibitors limit concomitant polysaccharide synthesis in the human gut symbiont Bacteroides fragilis. Proc. Natl. Acad. Sci. U. S. A. **107**:11976–11980.
36. **Coyne MJ, Chatzidaki-Livanis M, Paoletti LC, Comstock LE**. 2008. Role of glycan synthesis in colonization of the mammalian gut by the bacterial symbiont Bacteroides fragilis. Proc. Natl. Acad. Sci. U. S. A. **105**:13099–13104.
37. **Liu CH, Lee SM, VanLare JM, Kasper DL, Mazmanian SK**. 2008. Regulation of surface architecture by symbiotic bacteria mediates host colonization. Proc. Natl. Acad. Sci. **105**:3951–3956.
38. **Sara M, Sleytr UB**. 2000. S-Layer Proteins. J Bacteriol **182**:859–868.
39. **Sjogren A, Hovmoller S, Farrants G, Ranta H, Haapasalo M, Ranta K, Lounatmaa K**. 1985. Structures of two different surface layers found in six Bacteroides strains. J Bacteriol **164**:1278–1282.
40. **Every D, Skerman TM**. 1980. Ultrastructure of the Bacteroides nodosus cell envelope layers and surface. J Bacteriol **141**:845–857.
41. **Sabet M, Lee S-W, Nauman RK, Sims T, Um H-S**. 2003. The surface (S-) layer is a virulence factor of Bacteroides forsythus. Microbiology **149**:3617–3627.
42. **Fagan RP, Fairweather NF**. 2014. Biogenesis and functions of bacterial S-layers. Nat. Rev. Microbiol. **12**:211–222.

43. **Pumbwe L, Skilbeck CA, Wexler HM**. 2006. The Bacteroides fragilis cell envelope: Quarterback, linebacker, coach—or all three? Anaerobe **12**:211–220.
44. **Fletcher CM, Coyne MJ, Bentley DL, Villa OF, Comstock LE**. 2007. Phase-Variable Expression of a Family of Glycoproteins Imparts a Dynamic Surface to a Symbiont in Its Human Intestinal Ecosystem. Proc. Natl. Acad. Sci. **104**:2413–2418.
45. **Goodman AL, McNulty NP, Zhao Y, Leip D, Mitra RD, Lozupone CA, Knight R, Gordon JI**. 2009. Identifying Genetic Determinants Needed to Establish a Human Gut Symbiont in Its Habitat. Cell Host Microbe **6**:279–289.
46. **Schiebel E, Schwarz H, Braun V**. 1989. Subcellular location and unique secretion of the hemolysin of Serratia marcescens. J. Biol. Chem. **264**:16311–16320.
47. **Snyder JA, Lloyd AL, Lockatell CV, Johnson DE, Mobley HLT**. 2006. Role of Phase Variation of Type 1 Fimbriae in a Uropathogenic Escherichia coli Cystitis Isolate during Urinary Tract Infection. Infect. Immun. **74**:1387–1393.
48. **Troy EB, Carey VJ, Kasper DL, Comstock LE**. 2010. Orientations of the Bacteroides fragilis capsular polysaccharide biosynthesis locus promoters during symbiosis and infection. J. Bacteriol. **192**:5832–5836.
49. **Martens EC, Chiang HC, Gordon JI**. 2008. Mucosal Glycan Foraging Enhances Fitness and Transmission of a Saccharolytic Human Gut Bacterial Symbiont. Cell Host Microbe **4**:447–457.
50. **Institute VP, Laboratory SUA, Holdeman LV, Moore WEC**. 1975. Anaerobe Laboratory Manual. Virginia Polytechnic Institute and State University, Anaerobe Laboratory.
51. **Koropatkin NM, Martens EC, Gordon JI, Smith TJ**. 2008. Starch Catabolism by a Prominent Human Gut Symbiont Is Directed by the Recognition of Amylose Helices. Structure **16**:1105–1115.
52. **Gunther NW 4th, Snyder JA, Lockatell V, Blomfield I, Johnson DE, Mobley HLT**. 2002. Assessment of virulence of uropathogenic Escherichia coli type 1 fimbrial mutants in which the invertible element is phase-locked on or off. Infect. Immun. **70**:3344–3354.
53. **Moyes RB**. 2009. Fluorescent staining of bacteria: viability and antibody labeling. Curr. Protoc. Microbiol. **Appendix 3**:Appendix 3K.
54. **Sun Z, Kong J, Hu S, Kong W, Lu W, Liu W**. 2013. Characterization of a S-layer protein from Lactobacillus crispatus K313 and the domains responsible for binding to cell wall and adherence to collagen. Appl. Microbiol. Biotechnol. **97**:1941–1952.
55. **Ausiello CM, Cerquetti M, Fedele G, Spensieri F, Palazzo R, Nasso M, Frezza S, Mastrantonio P**. 2006. Surface layer proteins from Clostridium difficile induce inflammatory and regulatory cytokines in human monocytes and dendritic cells. Microbes Infect. **8**:2640–2646.
56. **Ryan A, Lynch M, Smith SM, Amu S, Nel HJ, McCoy CE, Dowling JK, Draper E, O'Reilly V, McCarthy C, O'Brien J, Ní Eidhin D, O'Connell MJ, Keogh B, Morton CO, Rogers TR, Fallon PG, O'Neill LA, Kelleher D, Loscher CE**. 2011. A Role for TLR4 in Clostridium difficile Infection and the Recognition of Surface Layer Proteins. PLoS Pathog **7**:e1002076.
57. **Calabi E, Calabi F, Phillips AD, Fairweather NF**. 2002. Binding of Clostridium difficile Surface Layer Proteins to Gastrointestinal Tissues. Infect Immun **70**:5770–5778.

58. **Emerson JE, Reynolds CB, Fagan RP, Shaw HA, Goulding D, Fairweather NF**. 2009. A novel genetic switch controls phase variable expression of CwpV, a Clostridium difficile cell wall protein. Mol. Microbiol. **74**:541–556.
59. **Reynolds CB, Emerson JE, de la Riva L, Fagan RP, Fairweather NF**. 2011. The Clostridium difficile Cell Wall Protein CwpV is Antigenically Variable between Strains, but Exhibits Conserved Aggregation-Promoting Function. PLoS Pathog **7**:e1002024.
60. **Thompson SA**. 2002. *Campylobacter* Surface-Layers (S-Layers) and Immune Evasion. Ann. Periodontol. **7**:43–53.
61. **Tu Z-C, Gaudreau C, Blaser MJ**. 2005. Mechanisms Underlying Campylobacter fetus Pathogenesis in Humans: Surface-Layer Protein Variation in Relapsing Infections. J. Infect. Dis. **191**:2082–2089.
62. **Sakakibara J, Nagano K, Murakami Y, Higuchi N, Nakamura H, Shimozato K, Yoshimura F**. 2007. Loss of adherence ability to human gingival epithelial cells in S-layer protein-deficient mutants of Tannerella forsythensis. Microbiology **153**:866–876.
63. **Munn CB, Ishiguro EE, Kay WW, Trust TJ**. 1982. Role of surface components in serum resistance of virulent Aeromonas salmonicida. Infect. Immun. **36**:1069–1075.
64. **Trust TJ, Ishiguro EE, Chart H, Kay WW**. 2009. VIRULENCE PROPERTIES OF Aeromonas salmonicida. J. World Maric. Soc. **14**:191–200.
65. **Phipps BM, Kay WW**. 1988. Immunoglobulin binding by the regular surface array of Aeromonas salmonicida. J. Biol. Chem. **263**:9298 –9303.
66. **Garduño RA, Moore AR, Olivier G, Lizama AL, Garduño E, Kay WW**. 2000. Host cell invasion and intracellular residence by *Aeromonas salmonicida*: Role of the S-layer. Can. J. Microbiol. **46**:660–668.
67. **Bjornson AB, Bjornson HS**. 1979. Participation of Immunoglobulin and the Alternative Complement Pathway in Opsonization of Bacteroides fragilis and Bacteroides thetaiotaomicron. Rev. Infect. Dis. **1**:347–356.
68. **Tofte RW, Peterson PK, Schmeling D, Bracke J, Kim Y, Quie PG**. 1980. Opsonization of Four Bacteroides Species: Role of the Classical Complement Pathway and Immunoglobulin. Infect. Immun. **27**:784–792.
69. **Joiner KA, Hawiger A, Gelfand JA**. 1981. Activation of the Alternative Complement Pathway by Blood Culture Isolates of Bacteroides fragilis. Infect. Immun. **34**:303–305.
70. **Blaser MJ, Smith PF, Kohler PF**. 1985. Susceptibility of Campylobacter isolates to the bactericidal activity of human serum. J. Infect. Dis. **151**:227–235.
71. **Blaser MJ, Smith PF, Repine JE, Joiner KA**. 1988. Pathogenesis of Campylobacter fetus infections. Failure of encapsulated Campylobacter fetus to bind C3b explains serum and phagocytosis resistance. J. Clin. Invest. **81**:1434–1444.
72. **Lambris JD, Ricklin D, Geisbrecht BV**. 2008. Complement evasion by human pathogens. Nat. Rev. Microbiol. **6**:132–142.
73. **Ahrenstedt O, Knutson L, Nilsson B, Nilsson-Ekdahl K, Odlind B, Hällgren R**. 1990. Enhanced local production of complement components in the small intestines of patients with Crohn's disease. N. Engl. J. Med. **322**:1345–1349.
74. **Baklien K, Brandtzaeg P**. 1974. IMMUNOHISTOCHEMICAL LOCALISATION OF COMPLEMENT IN INTESTINAL MUCOSA. The Lancet **304**:1087–1088.
75. **Halstensen TS, Brandtzaeg P**. 1991. Local complement activation in inflammatory bowel disease. Immunol. Res. **10**:485–492.

76. **Halstensen TS, Mollnes TE, Garred P, Fausa O, Brandtzaeg P**. 1992. Surface epithelium related activation of complement differs in Crohn's disease and ulcerative colitis. Gut **33**:902–908.
77. **Belzer C, Liu Q, Carroll MC, Bry L**. 2011. THE ROLE OF SPECIFIC IgG AND COMPLEMENT IN COMBATING A PRIMARY MUCOSAL INFECTION OF THE GUT EPITHELIUM. Eur. J. Microbiol. Immunol. **1**:311–318.
78. **Andoh A, Fujiyama Y, Sakumoto H, Uchihara H, Kimura T, Koyama S, Bamba T**. 1998. Detection of complement C3 and factor B gene expression in normal colorectal mucosa, adenomas and carcinomas. Clin. Exp. Immunol. **111**:477–483.
79. **Laufer J, Oren R, Goldberg I, Horwitz A, Kopolovic J, Chowers Y, Passwell JH**. 2000. Cellular localization of complement C3 and C4 transcripts in intestinal specimens from patients with Crohn's disease. Clin. Exp. Immunol. **120**:30–37.
80. **Chehoud C, Rafail S, Tyldsley AS, Seykora JT, Lambris JD, Grice EA**. 2013. Complement modulates the cutaneous microbiome and inflammatory milieu. Proc. Natl. Acad. Sci. **110**:15061–15066.
81. **Reinicke AT, Herrmann A, Baer F, Sina C, Srinivas G, Kuenzel S, Baines J, Köhl J**. 2012. C5aR regulates intestinal microbiota composition and controls the induction of gastrointestinal allergic hypersensitivity. XXIV Int. Complement Work. **217**:1147.
82. **Maekawa T, Krauss JL, Abe T, Jotwani R, Triantafilou M, Triantafilou K, Hashim A, Hoch S, Curtis MA, Nussbaum G, Lambris JD, Hajishengallis G**. 2014. Porphyromonas gingivalis Manipulates Complement and TLR Signaling to Uncouple Bacterial Clearance from Inflammation and Promote Dysbiosis. Cell Host Microbe **15**:768–778.
83. **Erridge C, Pridmore A, Eley A, Stewart J, Poxton IR**. 2004. Lipopolysaccharides of Bacteroides fragilis, Chlamydia trachomatis and Pseudomonas aeruginosa signal via Toll-like receptor 2. J. Med. Microbiol. **53**:735–740.
84. **Mancuso G, Midiri A, Biondo C, Beninati C, Gambuzza M, Macrì D, Bellantoni A, Weintraub A, Espevik T, Teti G**. 2005. Bacteroides fragilis-Derived Lipopolysaccharide Produces Cell Activation and Lethal Toxicity via Toll-Like Receptor 4. Infect. Immun. **73**:5620–5627.
85. **Alhawi M, Stewart J, Erridge C, Patrick S, Poxton IR**. 2009. Bacteroides fragilis signals through Toll-like receptor (TLR) 2 and not through TLR4. J. Med. Microbiol. **58**:1015–1022.
86. **Coats SR, Berezow AB, To TT, Jain S, Bainbridge BW, Banani KP, Darveau RP**. 2011. The Lipid A Phosphate Position Determines Differential Host Toll-Like Receptor 4 Responses to Phylogenetically Related Symbiotic and Pathogenic Bacteria. Infect. Immun. **79**:203–210.
87. **Macpherson AJ, Geuking MB, Slack E, Hapfelmeier S, McCoy KD**. 2012. The habitat, double life, citizenship, and forgetfulness of IgA. Immunol. Rev. **245**:132–146.
88. **Macpherson AJ, Uhr T**. 2004. Induction of Protective IgA by Intestinal Dendritic Cells Carrying Commensal Bacteria. Science **303**:1662–1665.
89. **Huang JY, Lee SM, Mazmanian SK**. 2011. The human commensal Bacteroides fragilis binds intestinal mucin. Anaerobe **17**:137–141.

90. **Johansson MEV, Hansson GC**. 2012. Preservation of Mucus in Histological Sections, Immunostaining of Mucins in Fixed Tissue, and Localization of Bacteria with FISH, p. 229–235. *In* McGuckin, MA, Thornton, DJ (eds.), Mucins. Humana Press.
91. **Johansson MEV, Phillipson M, Petersson J, Velcich A, Holm L, Hansson GC**. 2008. The inner of the two Muc2 mucin-dependent mucus layers in colon is devoid of bacteria. Proc. Natl. Acad. Sci. **105**:15064–15069.
92. **Eini A, Sol A, Coppenhagen-Glazer S, Skvirsky Y, Zini A, Bachrach G**. Oxygen deprivation affects the antimicrobial action of LL-37 as determined by microplate real-time kinetic measurements under anaerobic conditions. Anaerobe.
93. **Ogasawara H, Yamamoto K, Ishihama A**. 2011. Role of the Biofilm Master Regulator CsgD in Cross-Regulation between Biofilm Formation and Flagellar Synthesis. J. Bacteriol. **193**:2587–2597.
94. **Kuwahara T, Yamashita A, Hirakawa H, Nakayama H, Toh H, Okada N, Kuhara S, Hattori M, Hayashi T, Ohnishi Y**. 2004. Genomic analysis of Bacteroides fragilis reveals extensive DNA inversions regulating cell surface adaptation. Proc. Natl. Acad. Sci. U. S. A. **101**:14919–14924.